ERRATA

Technical Report No. 105

Page 19, Table II: "Percent Detection at 0.10 False Alarm" should read "Percent Detection at 0.10 Percent False Alarm;" and "99.82" should read "97.2."

Page 20, Section 4.1, second paragraph: "A/b^2" should read "s/b^2."

Page 22, Fig. 9: "$s/b = 2.5$" should read $s/b^2 = 2.5$."

Page 36, second line following Eq. (10): "...Eq. (9) represents..." should read "...Eq. (10) represents..."

THE UNIVERSITY OF MICHIGAN RESEARCH INSTITUTE
ANN ARBOR

STATISTICAL MEASUREMENTS OF THE DETECTION OF A CONTINUOUS SIGNAL BY A PANORAMIC RECEIVER

Technical Report No. 105

Electronic Defense Group
Department of Electrical Engineering

By: Q. C. Wilson, II
D. W. Fife

Approved by: A. B. Macnee

Project 2899

TASK ORDER NO. EDG-3
CONTRACT NO. DA-36-093 sc-78283
SIGNAL CORPS, DEPARTMENT OF THE ARMY
DEPARTMENT OF ARMY PROJECT NO. 3A 99-06-001-01

May 1960

TABLE OF CONTENTS

LIST OF ILLUSTRATIONS

LIST OF ILLUSTRATIONS (Cont.)

ABSTRACT

A simulated receiver capable of statistically measuring detection is used to investigate panoramic reception. The receiver includes an IF amplifier, a linear or square-law detector, and a video filter. In this mode of reception, the receiver repeatedly sweeps through a band of frequencies and records the distribution of the maximum amplitude of the video filter output. Sweep speed, observation time, signal-to-noise ratio, and video filter bandwidth are variables, while IF bandwidth enters as a normalization of the sweep speed. The data are presented in the form of "receiver operating characteristic curves," and the measure of detection is the parameter d'.

1. INTRODUCTION

This report describes the results of an experimental study to assess the influence of input signal-to-noise ratio, sweep rate, observation time, and video filter bandwidth on signal detection by a panoramic receiver. The receiver attempts to detect the presence of a continuous signal on the first sweep through the signal frequency. An analog technique using a statistical receiver (SIMRAR) is the tool for the investigation. An earlier report (Ref. 1) determined the effects of these parameters on the output signal-to-noise ratio of a panoramic receiver when the signal was a short pulse that occurred at the instant the receiver passed through the pulse frequency.

The simulation technique used here is the same as was used in the initial studies of a panoramic receiver (Ref. 2); i.e., the simulation takes place after an ideal mixer, with a linearly sweeping local oscillator. A received CW signal is therefore simulated by a linearly swept-frequency signal at the input to the IF amplifier; the wide-band white Gaussian noise at the receiver input is simulated by white Gaussian noise, very wide compared to the IF amplifier, added at the IF amplifier input. The signal is generated in an auxiliary swept-frequency signal generator, which together with SIMRAR is the total simulation. SIMRAR records the amplitude distribution of the receiver output, which, after a large number of detection trials, determines the receiver operating characteristic curve (ROC curve) (Ref. 3) for each setting of the

parameters. The ROC yields a more complete picture of detectability than output signal-to-noise ratio. When the curve is normal, the quality of detection is specified by the index d' (Ref. 4) that corresponds to that normal ROC.

2. PANORAMIC RECEIVER SIMULATION

2.1 SIMRAR (SIMulated Receiver and Recorder)

Experimental studies of detection by a panoramic receiver have been carried out using the SIMRAR equipment and a panoramic signal generator. Figure 1 is a block diagram of SIMRAR as used in panoramic receiver experiments. SIMRAR is an analog statistical receiver which alternately makes trials with signal-and-noise and noise-alone. The use of operational amplifiers, as shown in Figure 1, indicates that variable elements have been anticipated. The diode function generator permits simulation of arbitrary non-linear detector characteristics. The linear and square law detector have been considered in the present study.

SIMRAR handles real voltage signal peaks of about 60 volts throughout the signal path. The feedback amplifiers allow proper amplification scaling for a wide variety of signals. The threshold detectors are individually preset according to the expected distribution of the amplitude of the receiver output, and the counters record the number of trials, on each alternative, for which the receiver output exceeded the preset threshold value. A properly scaled 2kc perturbation signal, which is necessary for accurate recording, is added to the receiver output at the video amplifier. Additional counters record the total number of trials on each alternative.

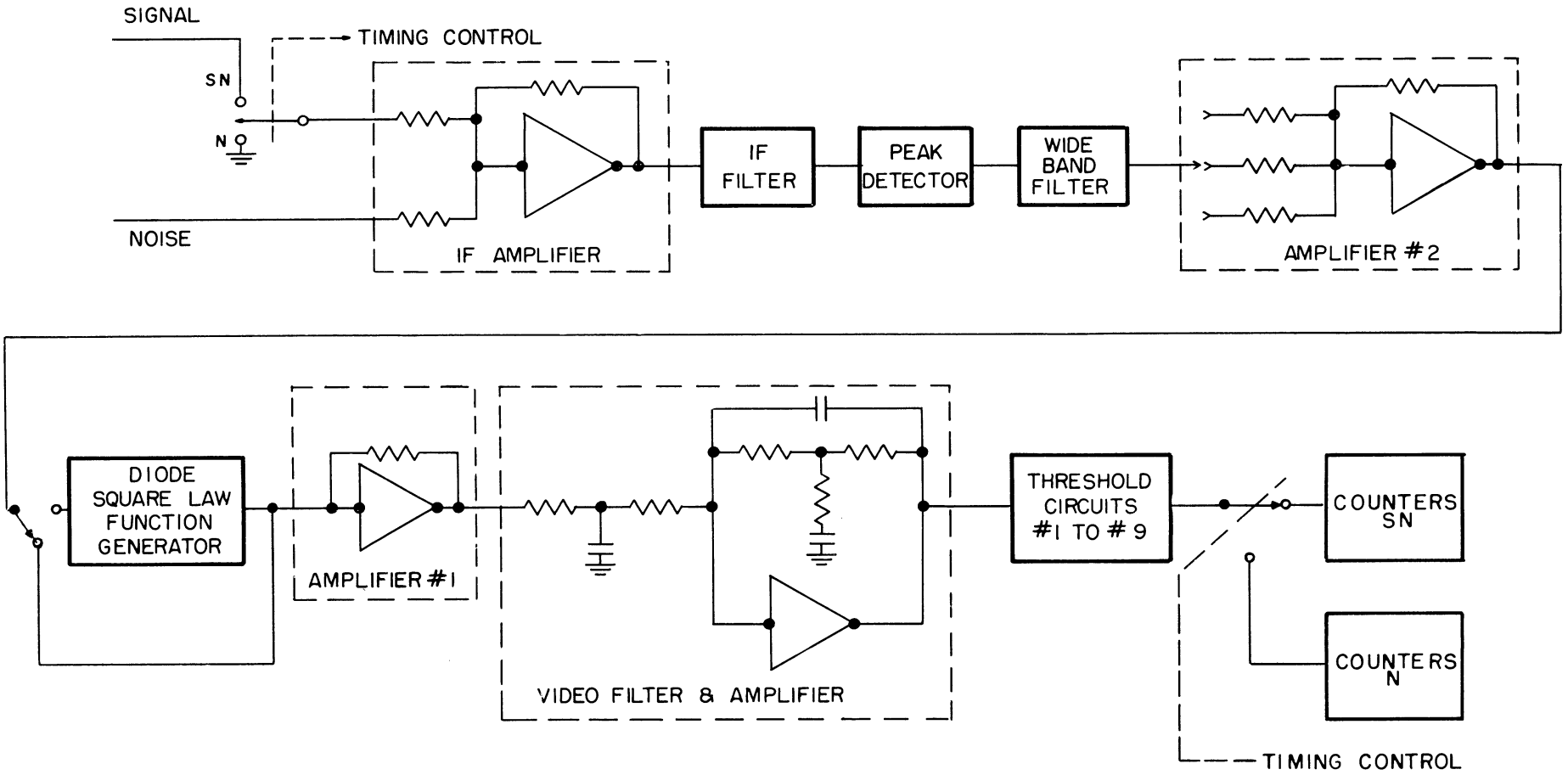

FIG. 1 SIMRAR AS USED IN PANORAMIC RECEIVER TESTING

Timing circuits control the time duration of the test interval, which is variable over a wide range. The timing circuits also fulfill several functions germane to the operation of the threshold detectors and counters, and alternate the input of the receiver between the signal-and-noise case and the noise-alone case.

The video filter bandwidth is varied by changing the capacitors in the filter network. The bandwidths used are 1/8, 1/4, 1/2, 1, and 2 times the IF bandwidth. The video amplifier gain can also be changed by changing the resistance values in the amplifier input. Figure 2 is a

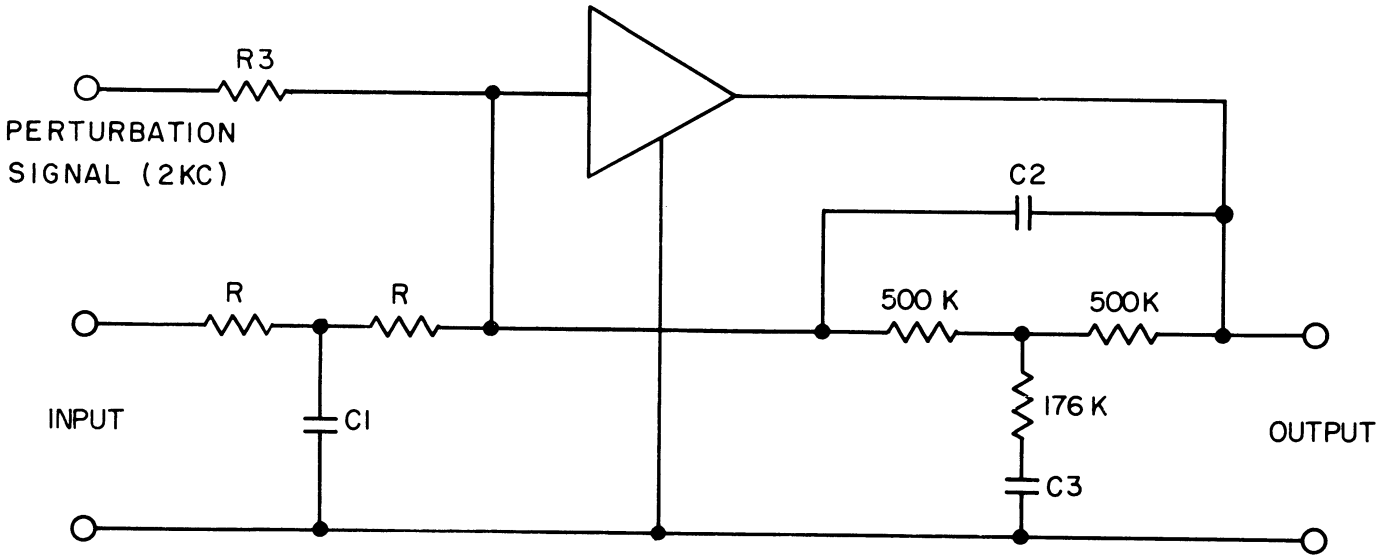

Fig. 2. Video Filter and Amplifier Schematic Diagram

schematic diagram of the video filter and amplifier. R_3 provides for proper scaling of the 2kc perturbation signal. The component values for the filter are given in Table I.

Figure 3 shows the connections for mating SIMRAR and the panoramic signal generator.

Several features of the SIMRAR equipment design minimize the effect of equipment drifts and inaccuracies which might otherwise be

TABLE I

COMPONENT VALUES FOR VIDEO FILTER

Bandwidth (cps)	Gain	C_1 μf	R Ω	C_2 μf	C_3 μf	Perturbation Resistor R_3 Ω
2.5	1	.254	500K	.0636	.1492	680K
	2	.508	250K			
	6	1.52	83.3K (100K and 500K in parallel)			
5.0	1	.1275	500K	.0319	.0747	1.5M and 1.8M in parallel
	2	.254	250K			
	6	.765	83.3K			
10	1	.0636	500K	.0159	.0374	5.6M and 8.2M in parallel
	2	.1275	250K			
	6	.382	83.3K			
20	1	.0318	500K	.00796	.0187	6.8M
	2	.0636	250K			
	6	.191	83.3K			
40	1	.0159	500K	.00398	.00934	4.7M and 22M in parallel
	2	.0318	250K			
	6	.0955	83.3K			

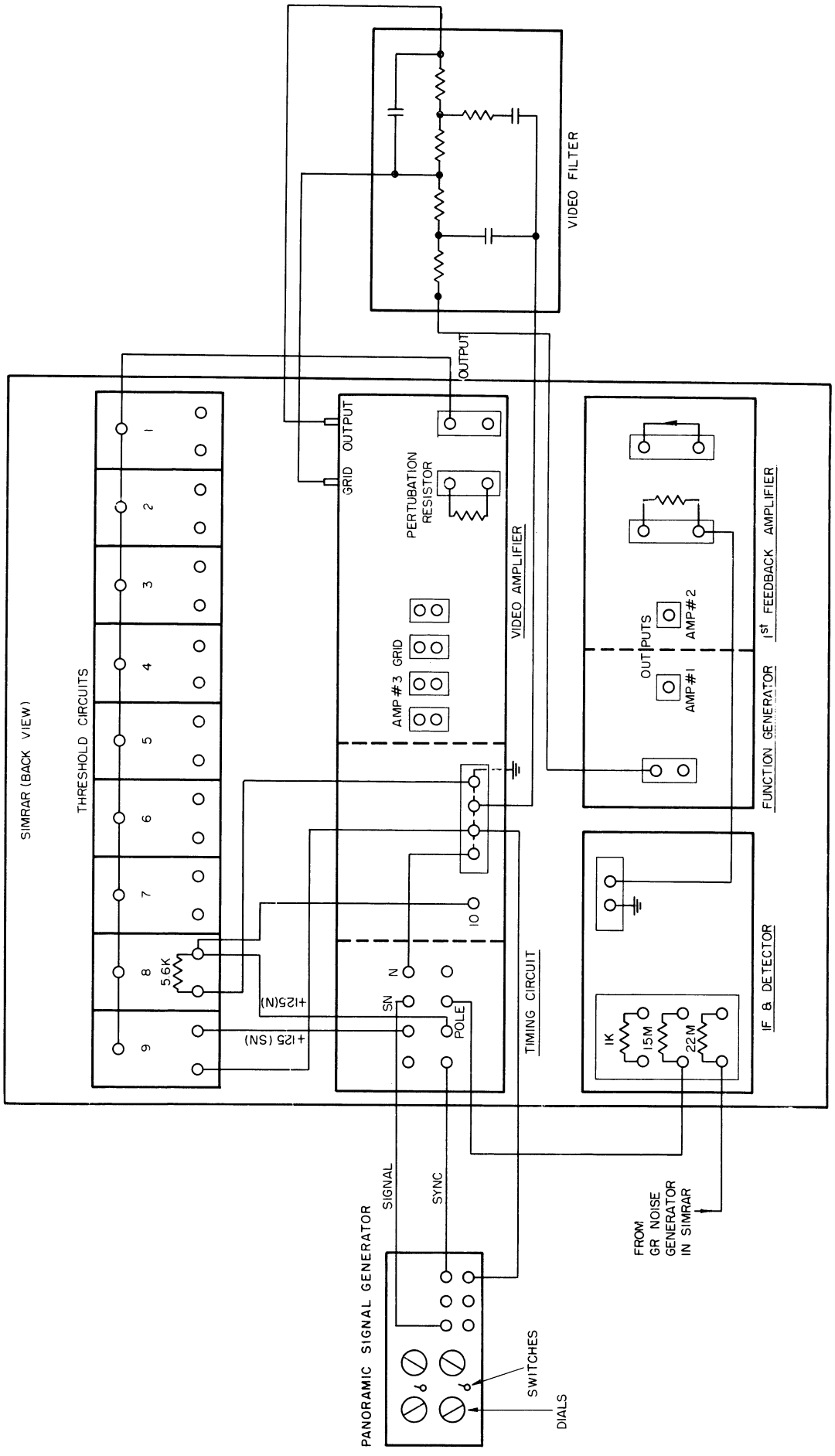

FIG. 3 SIMRAR PANORAMIC SIGNAL GENERATOR INTERCONNECTIONS

critical in statistical measurements. For example, the threshold circuits are common to both SN and N channels and are actuated by alternate switching of the power supply voltage. Inaccuracy in the threshold level setting and variations in dynamic behavior between alternatives is therefore eliminated. Consecutive alternation between trials with signal-and-noise and noise alone, minimizes the problems of long term drift in the equipment, which might be significant if data for either case alone were taken in one series of trials. In general, the exact threshold level is not important since the primary interest is the relative number of trials for signal-and-noise and noise alone on which the threshold is exceeded. Any drift in the equipment common to both channels only results in a shift of the data point along the receiver operating curve, yielding the same detection performance. The cumulative drift and inaccuracies in amplifiers and recording circuits, exclusive of the signal and noise sources, yield variations below 5 per cent. The observation time interval, as determined by the timing circuits, is sufficiently stable to present no significant variation in comparison.

The accuracy with which crossing of the threshold level is detected is improved by the use of the 2kc perturbation signal. This signal is scaled to approximately 100 millivolts, peak-to-peak, and rides along the top of the input waveform to the threshold circuits. When the threshold level is exceeded, the 2kc signal is gated into a bandpass amplifier, and the amplified signal triggers a thyratron. The counters are located in the plate circuits of the thyratrons. This technique makes accurate recording possible regardless of the slope with which the input waveform crosses the threshold. It is apparent, however, that the resolution of the threshold circuits is at least as large as the

amplitude of the perturbation signal. The resolution of the threshold circuits is approximately 150 millivolts while the full dynamic range is 60 volts. A change in amplitude of 150 millivolts will bring the counter pairs from zero counts to full counts over a large number of trials. The effect of the phase of the 2kc signal is negligible since the input waveforms are generally band-limited well below 2kc.

Repeatibility of data from SIMRAR is generally good, and is limited primarily by the number of trials taken and the stability of the signal source. The noise generator in SIMRAR has good stability over the usual running time and is not a significant source of variation.

2.2 Panoramic Signal Generator

The panoramic signal generator generates a constant amplitude signal of increasing frequency from about 300 to 3000 cps. The frequency sweep is linear in the region of the IF pass band of SIMRAR, but at the upper end of the frequency range the sweep speed decreases exponentially. The starting frequency of the sweep is adjustable between approximately 300-1000 cps; hence the time position of the signal response can be placed anywhere in the observation interval of SIMRAR. Normally, the signal generator is slaved to SIMRAR, and the sweep is initiated by SIMRAR, when a ground connection is removed in the signal generator sweep circuit. However, the equipment includes a timing circuit for operation independent of SIMRAR.

Figure 4 is a block diagram of the panoramic signal generator. A positive and a negative sawtooth voltage (+e and -e) are generated and connected to a SPDT switch circuit. The pole of the switch circuit is the input to an integrator. The output of the integrator is an increasing

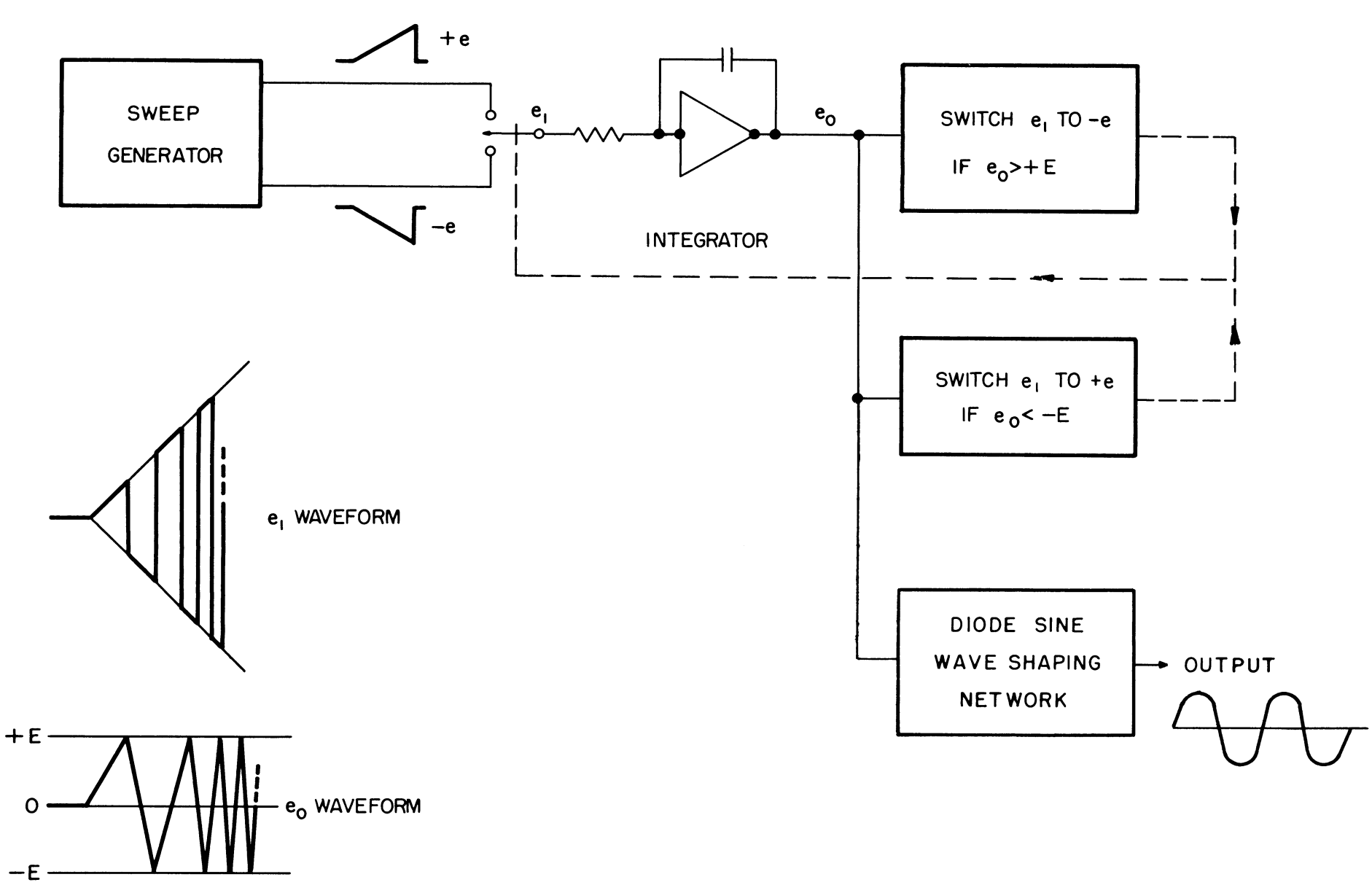

FIG. 4 BLOCK DIAGRAM OF PANORAMIC SIGNAL GENERATOR

frequency triangular waveform, which is shaped by the diode function generator to an approximately sinusoidal waveform.

A two-directional threshold detector controls the SPDT switch circuit. As the sawtooth waveforms, +e and -e, depart from zero voltage, the waveform at e_1 is a train of rectangles of slowly increasing amplitude. The slope of the waveform e_o is proportional to the amplitude of e_1. The threshold detector circuit changes the switch position when $|e_o| = E$, a constant, thereby reversing the direction of e_o. Thus e_o is a signal of nearly triangular shape and linearly increasing frequency. The rate of increase of frequency is controlled by the slope of the sawtooth voltages, +e and -e.

The next few paragraphs give a detailed description of the actual elements in the signal generator. The schematic diagram is Figure 5. The sawtooth waveforms, +e and -e, arise from symmetrical, oppositely-charging capacitor networks. Cathode followers set the voltage on one side of the capacitors. This voltage determines the starting frequency of the sweep. A balancing potentiometer adjusts the starting voltage so that it is of equal magnitude on both capacitor networks. Voltage regulator tubes are used to maintain the constant voltage across the charging networks. Thus the rate of rise of the sawtooth waveforms depends only on the RC time constant of the capacitor network. The time constant, and hence the sweep rate of the panoramic signal, is varied by switching capacitors in the network. The high impedance of the sweep circuits requires cathode followers for interstage isolation.

The SPDT switch circuit consists of six diodes intimately connected with the input to the integrator. It is driven at point A (see Figure 5) by a cathode follower with a square wave output alternating

between ± 70 volts. Consideration of the polarities of the diodes shows that a positive voltage at A grounds -e but does allow +e to be applied to the integrator.

The integrator is a push-pull two stage circuit using a differential amplifier and a cathode follower pair. Positive feedback is used to bring the amplifier to a psuedo-infinite gain condition. Capacitive feedback converts the amplifier into an integrator. The differential amplifier is balanced with a potentiometer. This eliminates skewness of the triangular output. Adjustment of the feedback potentiometer straightens the integrator output into linear segments.

The two-directional threshold circuit is a simple bistable multivibrator, which is triggered by the triangular integrator output. The output from one plate of the multivibrator drives the cathode follower, providing the switching voltage at A.

A potentiometer is used to adjust the triangular input to the diode shaping network to 26 volts peak. The shaping network uses high back-resistance crystal diodes and mercury cells as reference voltages. The output of the shaping circuit is a nearly sinusoidal waveform.

A simple dc amplifier and a cathode follower form the output stages of the panoramic signal generator. The remaining circuitry provides cyclic timing either through the synchronization action from SIMRAR or by an adjustable Schmidt-trigger threshold detector which is driven by the positive sawtooth waveform, +e. For operational convenience, one can select either of two preset starting frequencies and Schmidt-trigger thresholds by operating a lever switch.

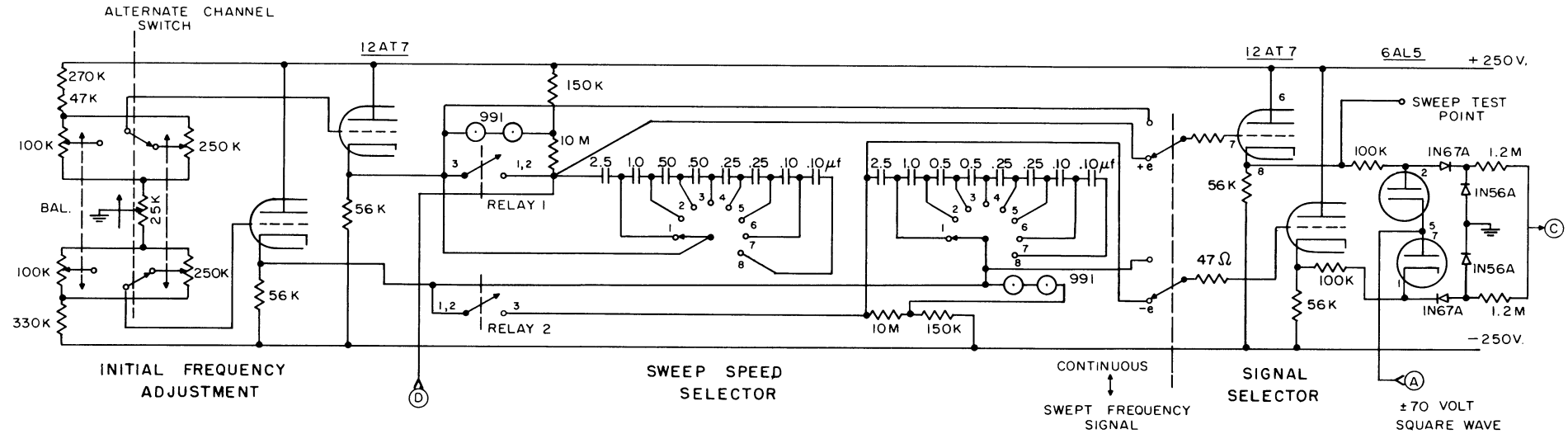

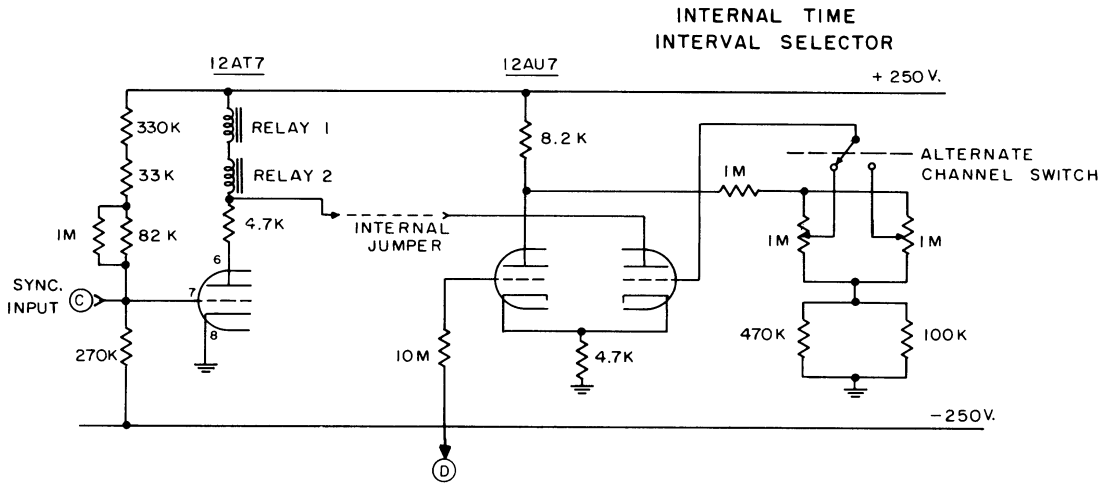

FIG. 5 PANORAMIC SIGNAL GENERATOR SCHEMATIC

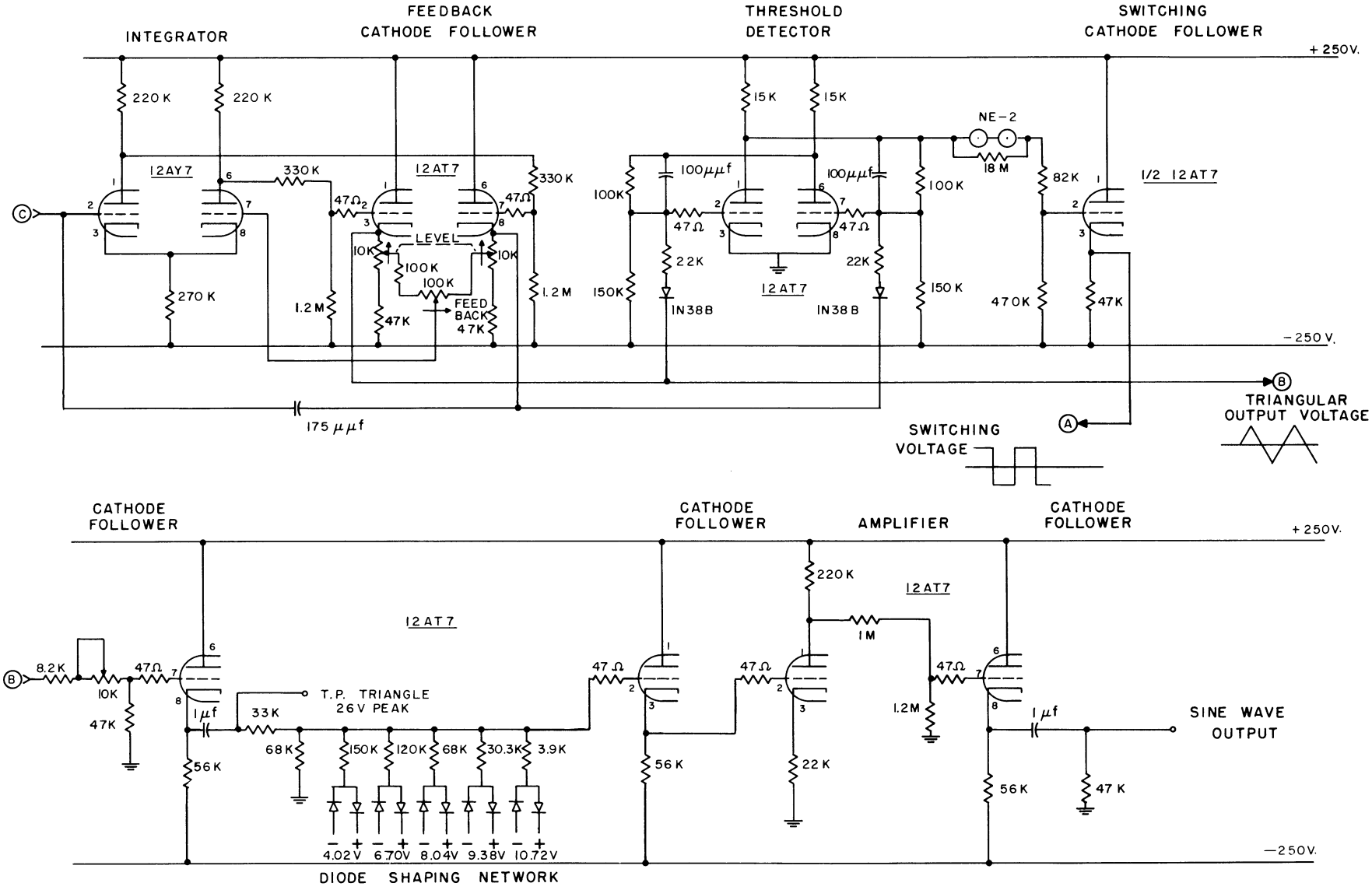
INTEGRATOR
FEEDBACK CATHODE FOLLOWER
THRESHOLD DETECTOR
SWITCHING CATHODE FOLLOWER
+250V.
220 K
220 K
12AY7
330K
12AT7
330K
47Ω
47Ω
LEVEL
10K
100K
100K
10K
270 K
1.2M
47K
FEED BACK 47K
1.2M
175 μμf
15K
15K
NE-2
18 M
100μμf
100μμf
100K
47Ω
47Ω
22K
22K
150K
12AT7
IN38B
IN38B
100K
150K
82K
1/2 12AT7
470K
47K
-250 V.
TRIANGULAR OUTPUT VOLTAGE
SWITCHING VOLTAGE
CATHODE FOLLOWER
CATHODE FOLLOWER
AMPLIFIER
CATHODE FOLLOWER
+250V.
12AT7
12AT7
220K
1M
8.2K
47Ω
10K
47K
1μf
33K
T.P. TRIANGLE 26V PEAK
68K
150K
120K
68K
30.3K
3.9K
56K
47Ω
47Ω
47Ω
56K
22K
1.2M
1μf
SINE WAVE OUTPUT
56K
47 K
4.02V
6.70V
8.04V
9.38V
10.72V
DIODE SHAPING NETWORK
-250V.

3. DATA COLLECTION

In this simulation SIMRAR measures the amplitude distribution of the peak video voltage over many detection trials, alternately making a signal-and-noise trial and a noise-alone trial. After a sufficiently large number of trials (400 to 2000), the counters of SIMRAR yield good estimates of the probabilities,

$$P_{SN}\ (\text{video amplitude} \geq a) = P_{SN}(A);\ \text{and}$$

$$P_{N}\ (\text{video amplitude} \geq a) = P_{N}(A).$$

That is, they give data for the receiver operating curve (ROC) for the particular conditions of sweep speed, video bandwidth, etc. that apply. In this study these curves are plotted on normal-normal probability paper.

For example, if 2000 sweeps (trials) were to constitute a run, 1000 sweeps would be with signal-and-noise, and 1000 sweeps would be with noise alone. Each threshold circuit of SIMRAR would control two counters alternately. A counter activated during signal-and-noise trials might read 340 after 1000 trials, while a counter activated during noise trials might read 120. This datum point of 34 per cent detection at 12 per cent false alarm would be entered on the normal-normal probability plot, and together with the points from the other counter pairs would form the ROC for the particular receiver parameters which were used on that run.

If the probability distribution functions, $P_{SN}(A)$ and $P_{N}(A)$, are both normal, the ROC is a straight line on the normal-normal plot. The slope of the straight line ROC is an indication of the relative magnitude of the standard deviations of the two distributions. Where the slope is greater than unity, $\sigma_{SN} < \sigma_{N}$; if the slope is exactly unity, $\sigma_{SN} = \sigma_{N}$;

and if the slope is less than unity, $\sigma_{SN} > \sigma_N$. An example of a panoramic receiver operating curve is shown in Figure 6a. The ROC's for these experiments were found to be of nearly unit slope. Therefore, a single measure of detection performance is the d' value corresponding to the point on the ROC with equal conditional errors. This quantity is the difference of the mean values of the $P_{SN}(A)$ and $P_N(A)$ probability distributions, and is a sufficiently accurate measure for this investigation. The results will be expressed primarily in terms of d'.

The accuracy of statistical measurements, even with perfect equipment, depends upon the number of trials taken. If the true probability of detection is p, and n independent trials are taken to measure this probability, the measured probability will have a standard deviation

$$\sigma = \sqrt{\frac{p\,(1-p)}{n}} \qquad (1)$$

from the true probability. This, of course, also applies to measurements of false alarm probability. Using Eq. (1), a region can be determined about an individual point on the true ROC within which the measured point will fall with a given probability. Figure 6b shows the 3σ regions, corresponding to an 99-1/2 per cent probability, for the true ROC with d' = 2 and 500 trials per alternative constituting the measurement. As the d' value of the true ROC diminishes, the possible dispersion normal to the true ROC becomes uniform along the ROC. As the d' value increases, the lines defining the region for the ROC become more curved, and much greater dispersion is possible at the extremes than at the middle of the ROC. In the present experiments, the individual points on the ROC are not determined independently; rather, each series of trials determines 10 points which form the ROC. Thus, the possible dispersion of points as a

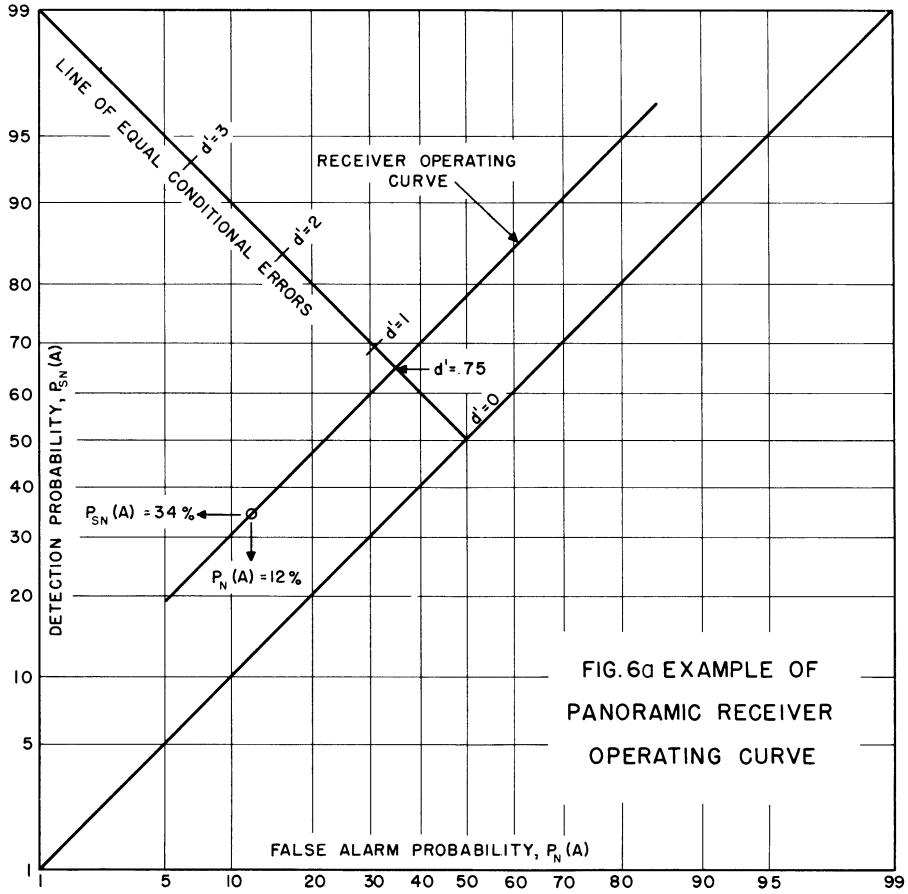

FIG. 6a EXAMPLE OF PANORAMIC RECEIVER OPERATING CURVE

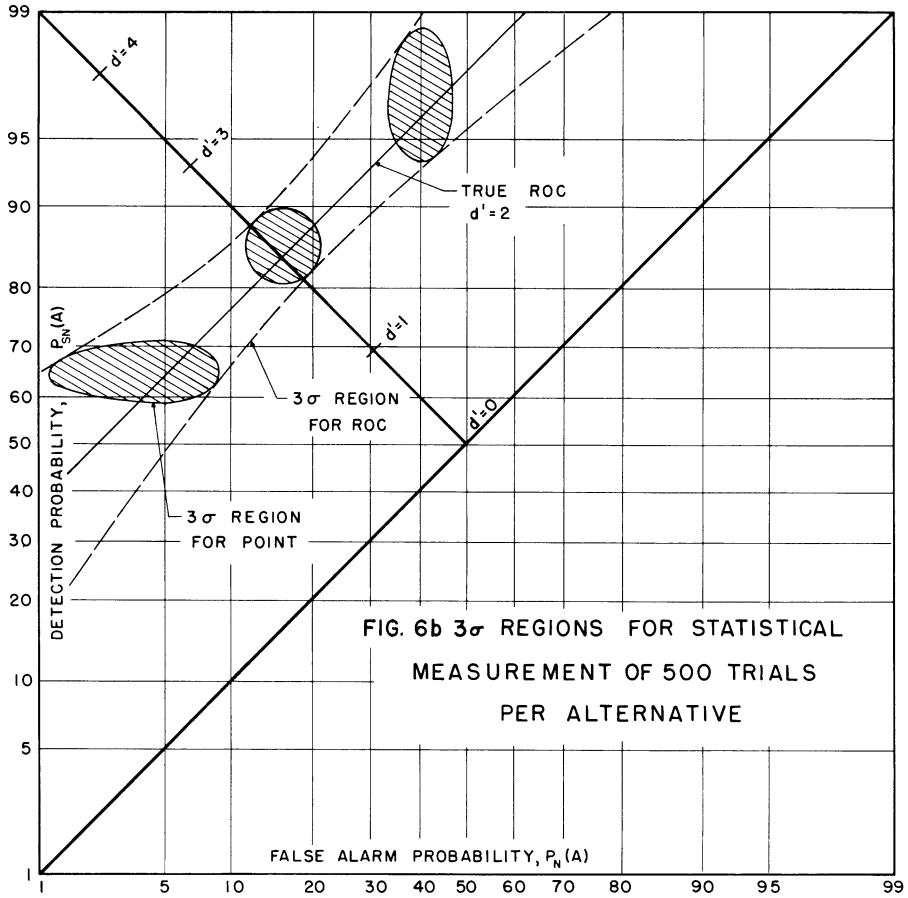

FIG. 6b 3σ REGIONS FOR STATISTICAL MEASUREMENT OF 500 TRIALS PER ALTERNATIVE

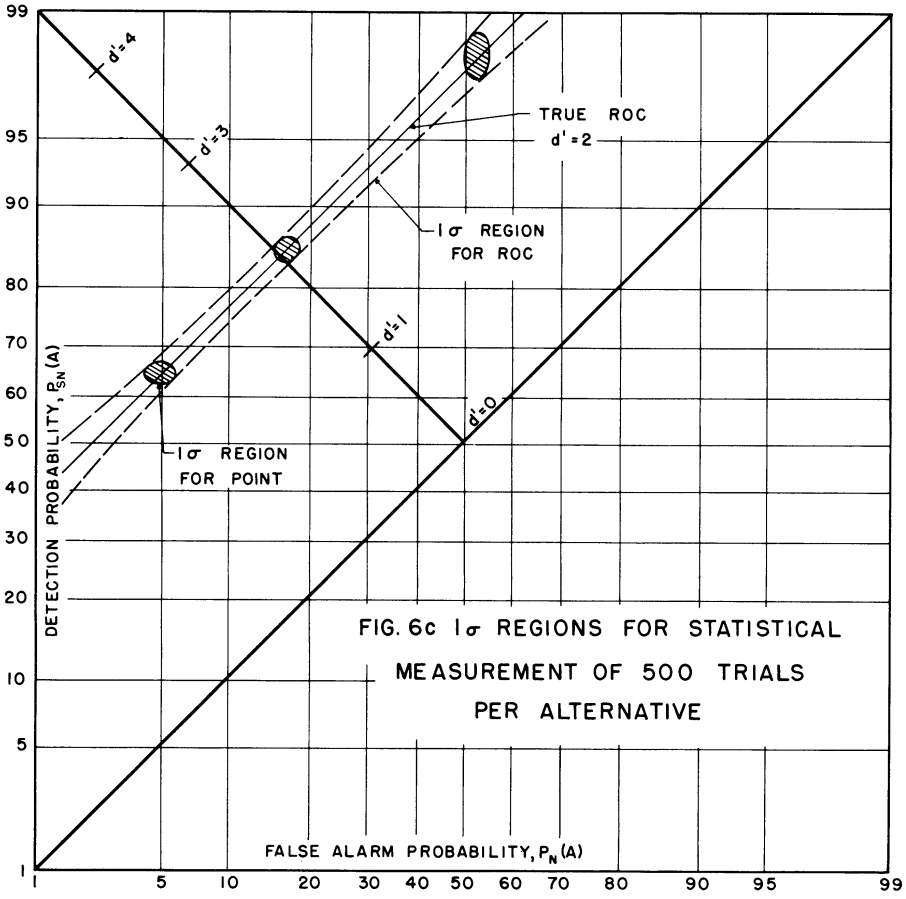

FIG. 6c 1σ REGIONS FOR STATISTICAL MEASUREMENT OF 500 TRIALS PER ALTERNATIVE

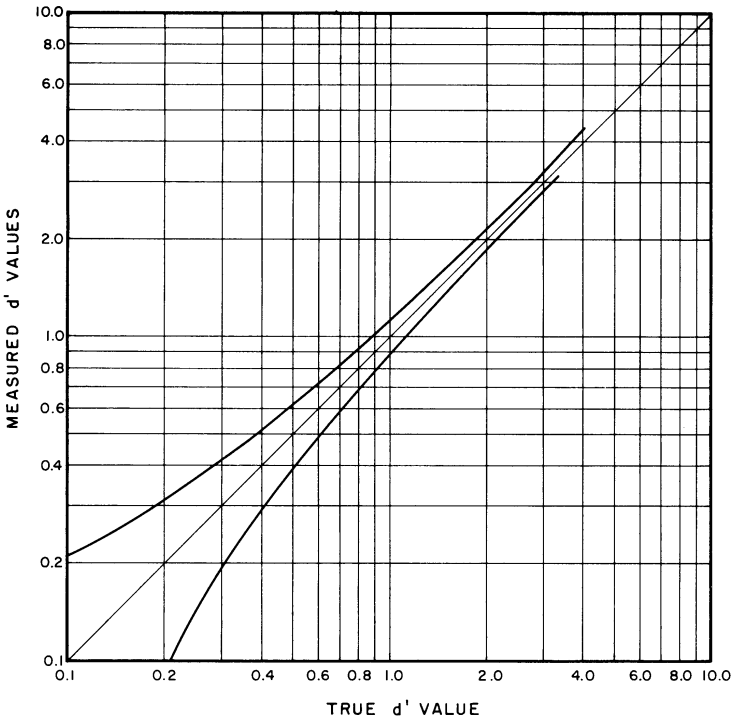

FIG. 6d 1σ RANGE OF MEASURED d' FOR EQUAL CONDITIONAL ERRORS, 500 TRIALS PER ALTERNATIVE

result of the number of trials taken is constrained to be more or less on one side or the other of the true ROC. Figure 6b demonstrates, however, that the statistical inaccuracy of a practical measurement may be the largest source of error. Figure 6c shows the 1σ regions, corresponding to 46-1/2 per cent probability, for the same case. Figure 6d shows the 1σ region of measured d' values on the line of equal conditional errors as a function of the true d' value for a single point. As mentioned above, this is somewhat pessimistic since the measured ROC is determined by several points taken simultaneously.

Most of the time spent in setting up a test is for adjusting the amplitude of the signals to make possible the use of a reasonable portion of the range of the threshold detectors in SIMRAR. The problem becomes severe with high d' values. Practically, a d' of five is very difficult to attain, the reason being that as performance nears perfect detection, the number of "mistakes" falls off sharply. In a run of 2000 sweeps, a mid-range counter will average 134 counts at d' = 3, 45.5 counts at d' = 4, 12.5 counts at d' = 5, and only 2.7 counts at d' = 6. Obviously, data above d' = 5 will require an excessive number of sweeps (10,000 or better) to obtain reasonable accuracy. The minimum dependable d' is about 0.2. Table II may help to clarify the extent of this range. Three normal ROC's are described in the table. The column listed S/N is the signal-to-noise ratio, out of a matched filter, necessary to achieve the performance characterized by the ROC.

Table III gives the range of variation of the receiver parameters which can readily be accomodated by the simulation. Note that the frequency band swept by the simulated receiver is the sweep rate multiplied by the observation time. The signal-to-noise ratio parameter, S/N,

TABLE II

OUTPUT S/N EQUIVALENT TO d'

d'	Percent Detection at 0.10 False Alarm	Percent Detection for Percent False Alarm = Percent Miss	Output S/N
0.2	0.19	54.00	-14 db
1.0	1.83	69.00	0 db
5.0	99.82	99.38	+14 db

TABLE III

RANGE OF PARAMETER VARIATION

Parameter	Range of Variation
Normalized Sweep Rate, s/b^2	0.1, 0.3, 0.6, 1.1, 1.8, 2.5, 4.6
Observation Time, T_o	0.1 to 3.0 sec
Video Bandwidth β	2.5, 5.0, 10.0, 20.0, 40.0 cps
Signal-Noise Ratio, S/N	2.5 to 47
Detection Measure, d'	0.2 to 4.0

is the ratio of peak signal power to noise power measured at the output of the IF filter, with the signal frequency constant and equal to the IF filter center frequency.

4. RESULTS OF DETECTION STUDIES

4.1 Receiver Operating Curves

A detailed mapping of panoramic receiver detection covering all possible combinations of sweep speed, sweep duration, signal-to-noise ratio, and video bandwidth would be unnecessarily time consuming. In this study the prominent features of the map have been explored by determining the effect of variation of each parameter, with others held constant. Several values of the other parameters have been used in this approach in order to reveal any unexpected trends. The results will be presented primarily in terms of the detection measure d', but included here are several figures illustrating the change in the ROC due to variation of each parameter.

Figures 7, 8, 9, and 10 give representative ROC's for variable S/N, A/b^2, T_o, and β, respectively, for the square law detector. ROC's for the linear detector are similar.

4.2 Measure of Detection, d'

The principal results of the signal detection studies presented here are the d' values of the point on the ROC with equal conditional errors, plotted against each of the variable parameters of the receiver. The data points obtained experimentally fit a straight line on a log-log plot with good accuracy in all cases, and the straight line fit is applied

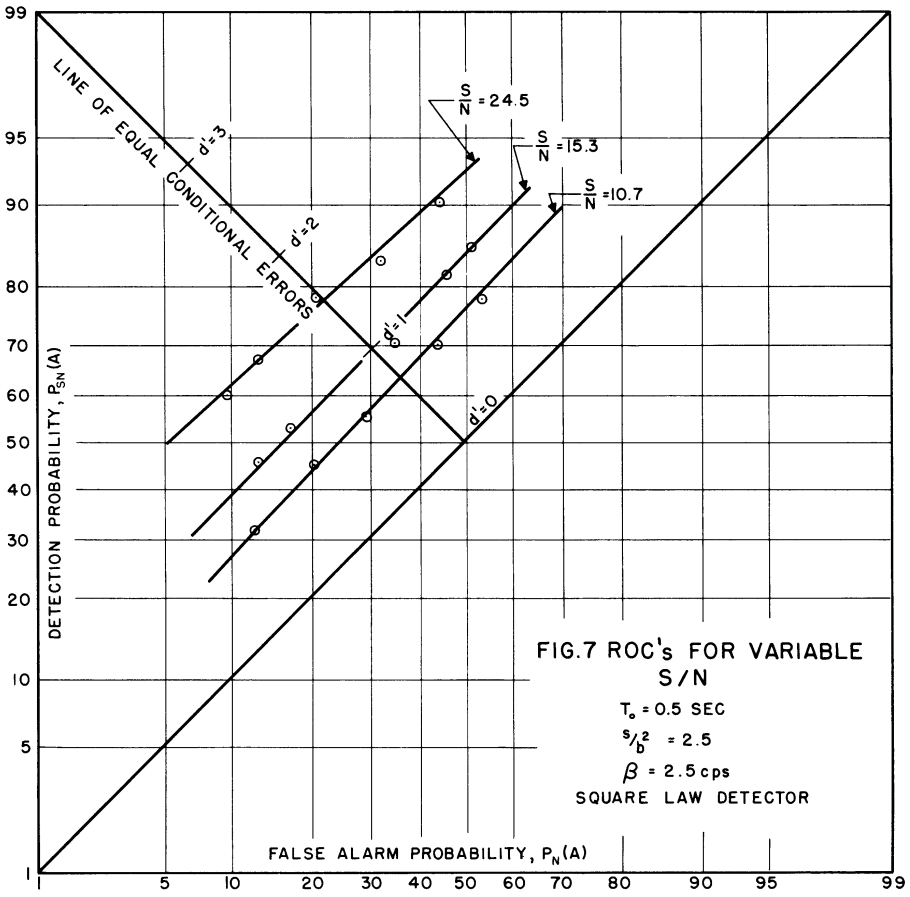

FIG.7 ROC's FOR VARIABLE S/N

T_o = 0.5 SEC

S/b^2 = 2.5

β = 2.5 cps

SQUARE LAW DETECTOR

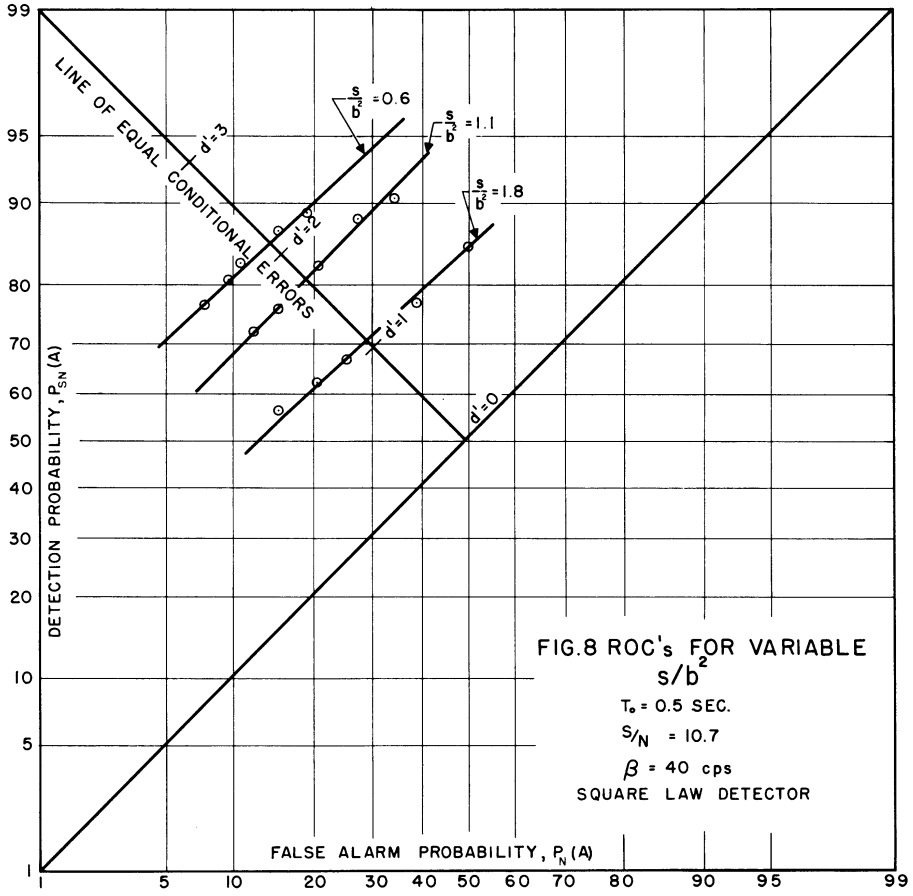

FIG.8 ROC's FOR VARIABLE s/b^2

T_o = 0.5 SEC.

S/N = 10.7

β = 40 cps

SQUARE LAW DETECTOR

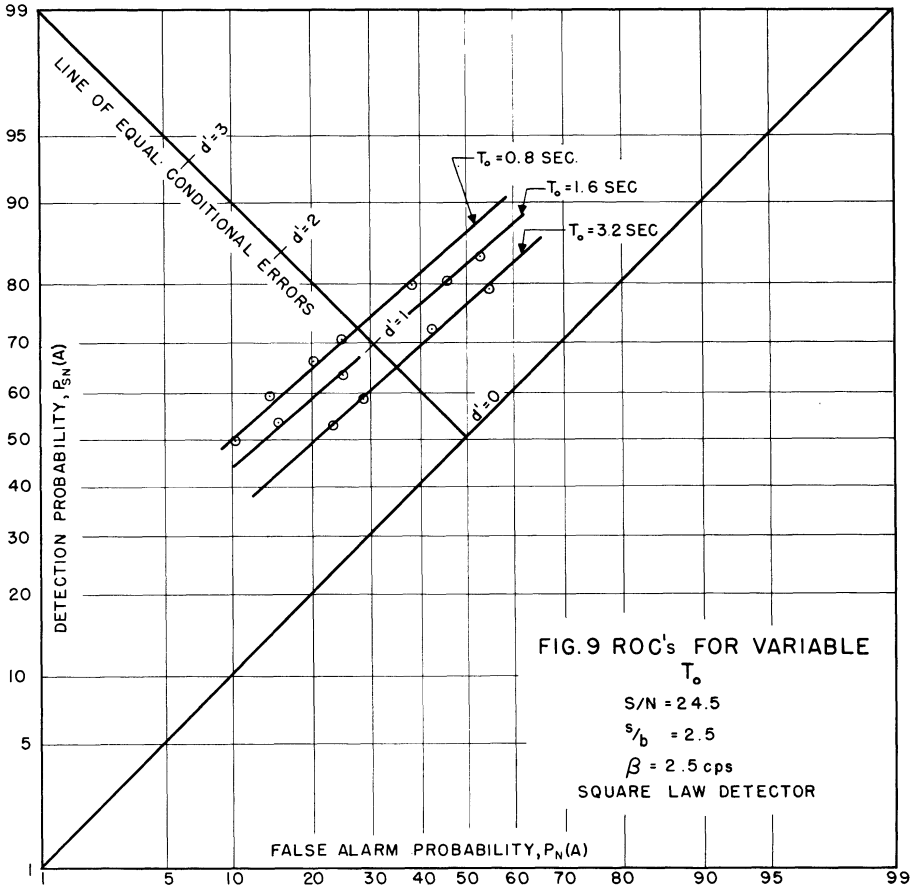

FIG. 9 ROC's FOR VARIABLE T_o

S/N = 24.5

S/b = 2.5

β = 2.5 cps

SQUARE LAW DETECTOR

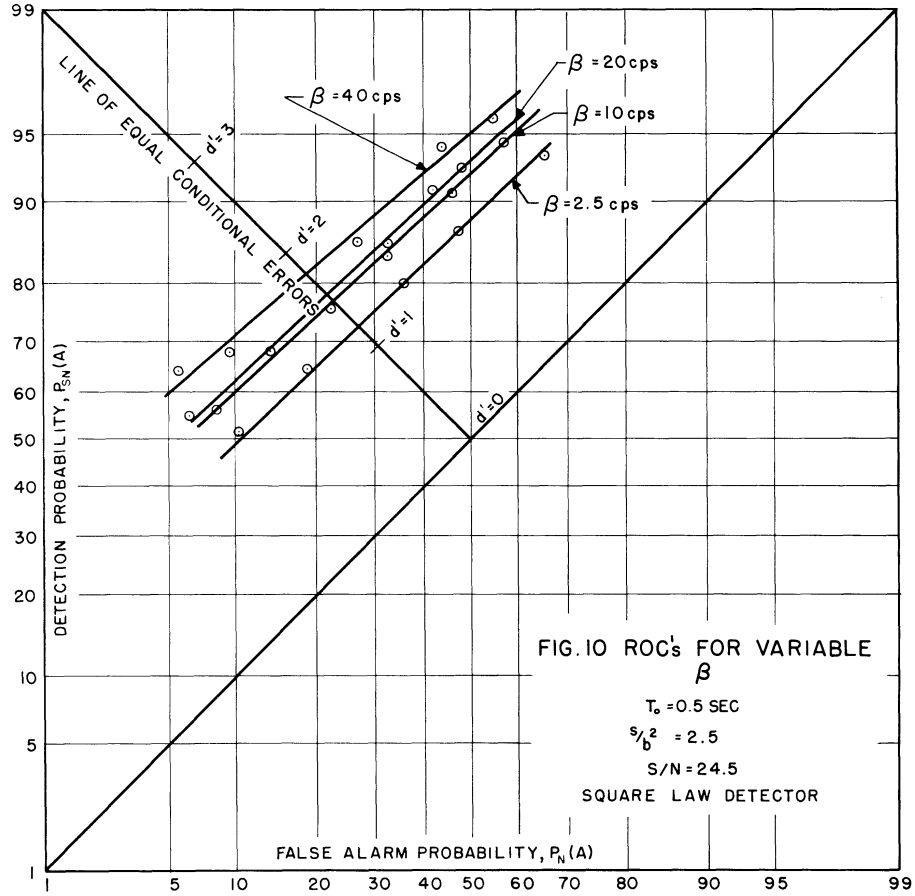

FIG. 10 ROC's FOR VARIABLE β

T_o = 0.5 SEC

S/b^2 = 2.5

S/N = 24.5

SQUARE LAW DETECTOR

to the data points for each variable parameter. Consequently, some discrepancy may be noted in the d' value for a particular set of conditions which appear on several plots on each of which the variable parameter is different. Such discrepancies fall within the limits of accuracy imposed by the simulation equipment and the number of detection trials taken.

4.2.1 d' as Function of Signal-to-Noise Ratio, S/N

Figures 11 and 12 show the variation in d', due to a change in the S/N power ratio, for the linear and square law detector. Curves are given for the wide and narrow video bandwidths and for low and high sweep speeds. d' values are slightly higher for the square law detector at the higher sweep speed than for the linear detector. The accuracy expected in the data leads to only the observation that at the lower sweep speed, the linear and square law detector perform nearly equally well, with the square law detector perhaps somewhat better. At the higher sweep speed, the wide video is better than the narrow video, while at the lower sweep speed the situation is reversed for the square law detector. The filters perform equally well at the low sweep speed for the linear detector.

The mode of variation of d' is apparently the same for both detector cases and is independent of sweep speed or video bandwidth. The relationship is very close to being linear,

$$d' \propto \frac{S}{N} . \qquad (2)$$

4.2.2 d' as a Function of Observation Interval, T_o

Figures 13 through 16 are plots of d' versus observation time

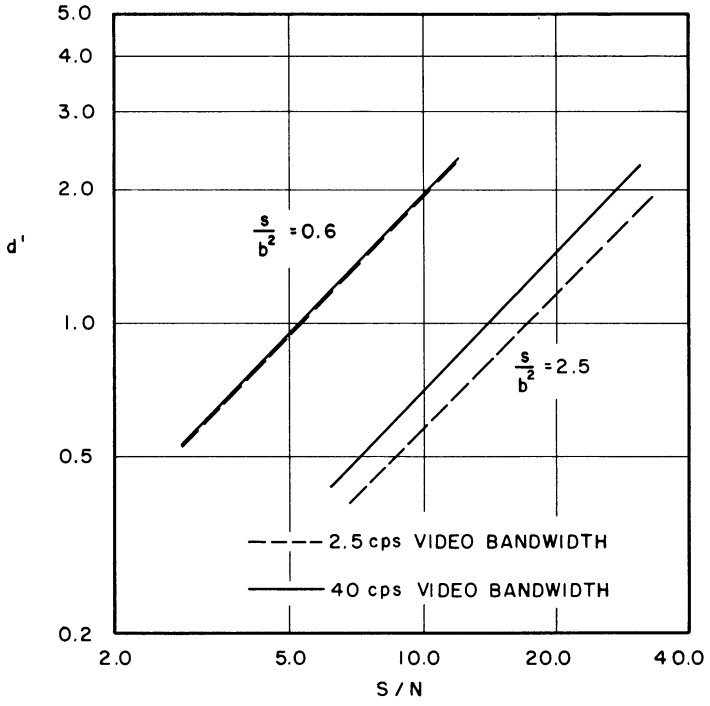

FIG. 11 d' vs. SIGNAL-TO-NOISE POWER RATIO, $\frac{S}{N}$

LINEAR DETECTOR
T_o =0.5 SEC

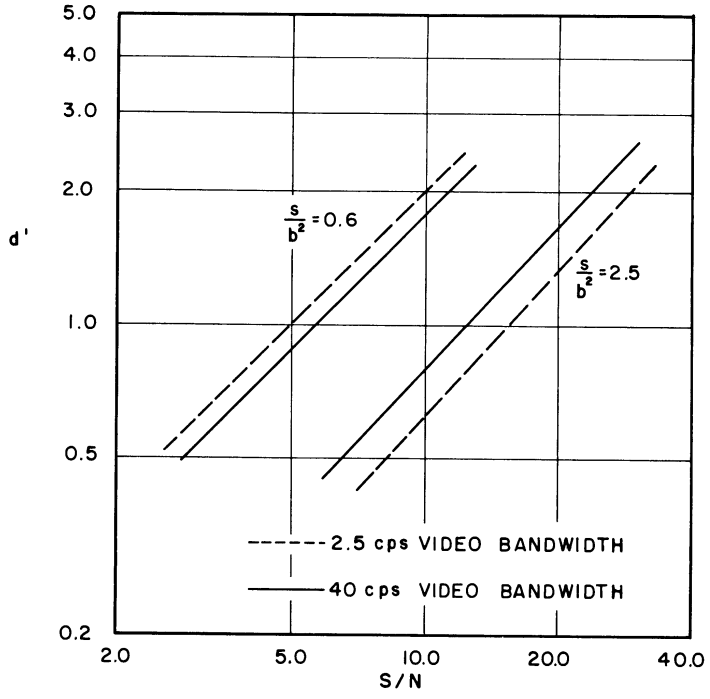

FIG. 12 d' vs. SIGNAL-TO-NOISE POWER RATIO, $\frac{S}{N}$

SQUARE LAW DETECTOR
T_o =0.5 SEC

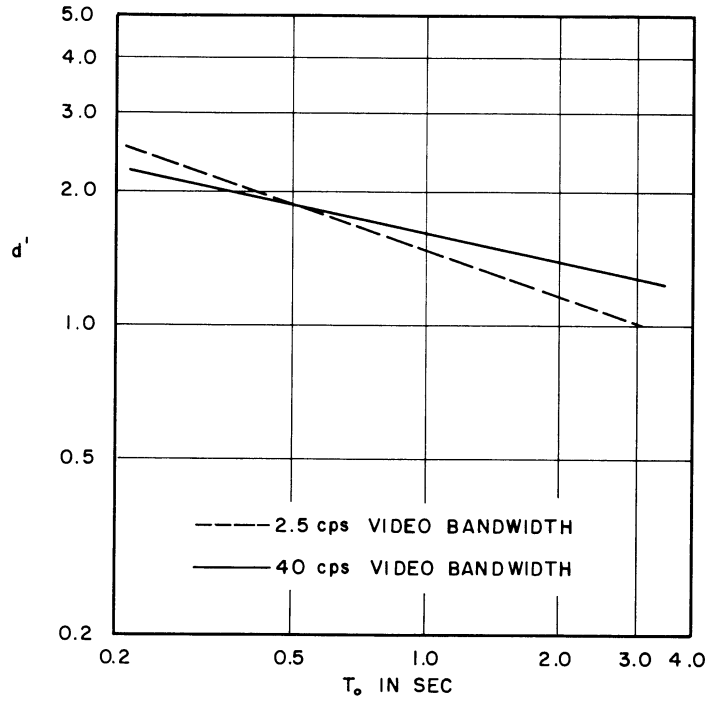

FIG. 13 d' vs. OBSERVATION TIME INTERVAL, T_o

LINEAR DETECTOR
S/N = 10.7
s/b^2 = 0.6

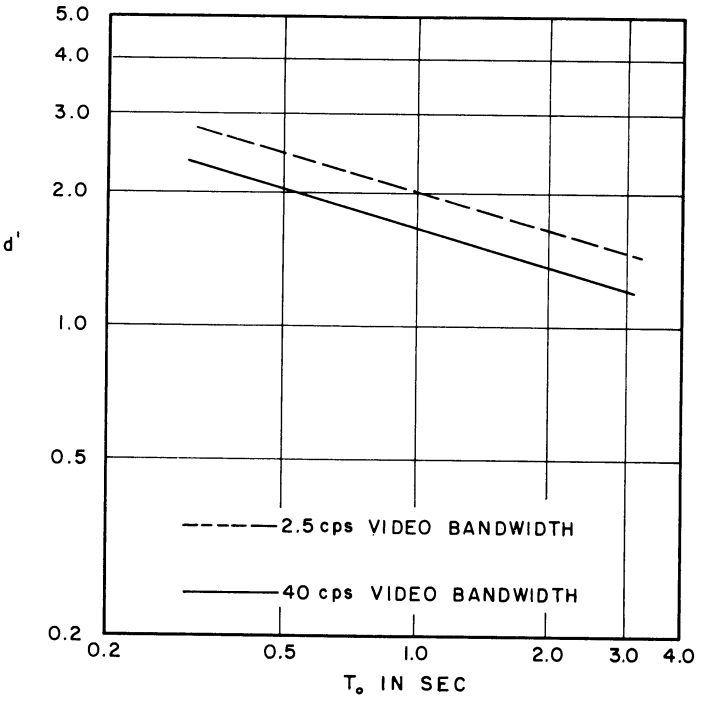

FIG. 14 d' vs. OBSERVATION TIME INTERVAL, T_o

SQUARE LAW DETECTOR
S/N = 10.7
s/b^2 = 0.6

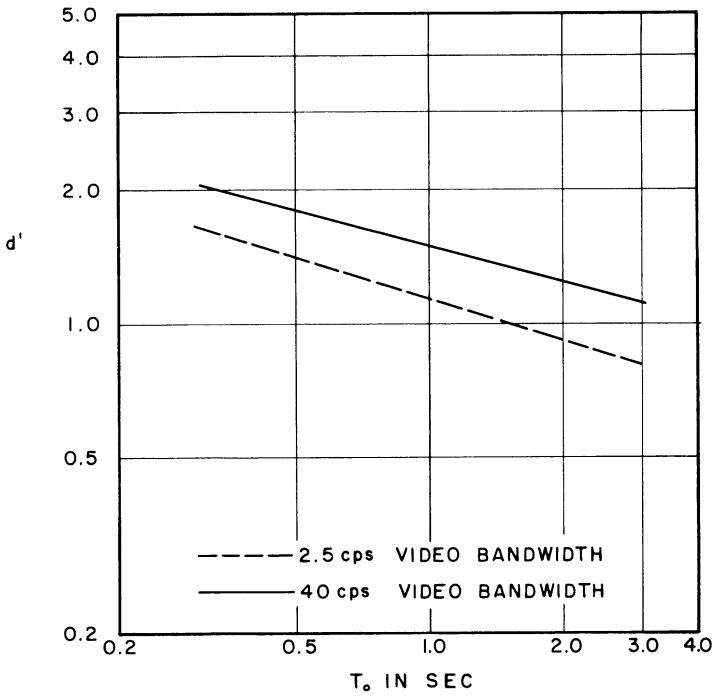

FIG. 15 d' vs. OBSERVATION TIME INTERVAL, T_o

LINEAR DETECTOR
S/N = 24.5
$s/b^2 = 2.5$

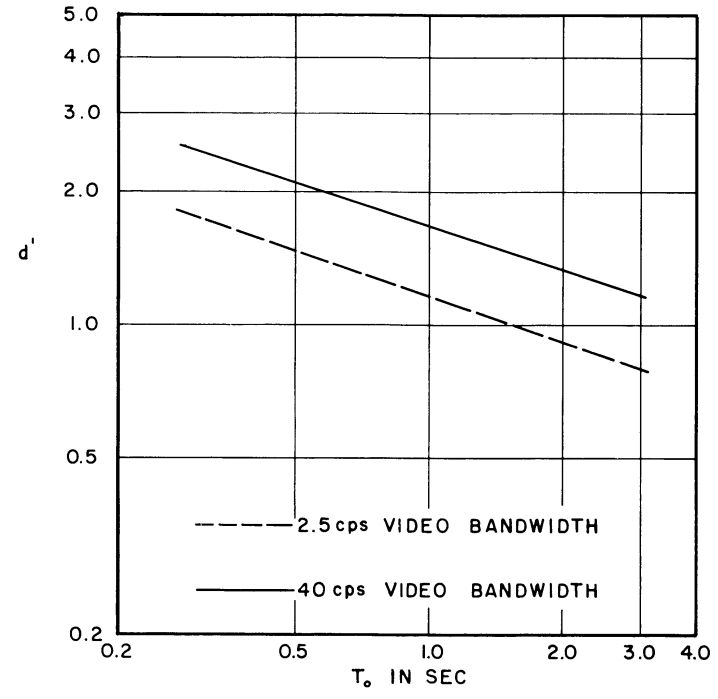

FIG. 16 d' vs. OBSERVATION TIME INTERVAL, T_o

SQUARE LAW DETECTOR
S/N = 24.5
$s/b^2 = 2.5$

interval for the two detector cases. Figures 13 and 14 show the variation at low sweep speed, and Figures 15 and 16 are for the higher sweep speed, $\frac{s}{b^2} = 2.5$.

In these curves, d' decreases as observation time increases. Also, it is not a bad approximation to say that d' decreases at the same rate, independent of the detector characteristic, sweep speed, or video bandwidth. Allowing this approximation, the relationship is

$$d' \propto (T_o)^{-\frac{1}{3}} . \qquad (3)$$

Figure 13 indicates that a selection between the two video filter bandwidths shown for best signal detection with a linear detector will depend upon the observation time interval at the low sweep speed. Actually, it will be seen from other curves that a selection between the two filters for either detector characteristic will depend upon sweep speed and observation time interval. It is only in Figure 13, however, that the crossover point between the two choices appears as a function of T_o.

4.2.3 d' as a Function of Normalized Sweep Speed, $\frac{s}{b^2}$

Figures 17 through 20 are plots of d' against the normalized sweep speed for the linear and square law detector cases. Plots for two observation time intervals, relatively short and long duration, are given.

It is observed at once that for both detector cases the wide video filter yields better detection at high sweep speeds, while the narrow bandwidth filter gives better detection at low sweep speeds. The value of sweep speed for which the two filters perform equally well, however, depends upon the observation time interval, it being lower for the longer

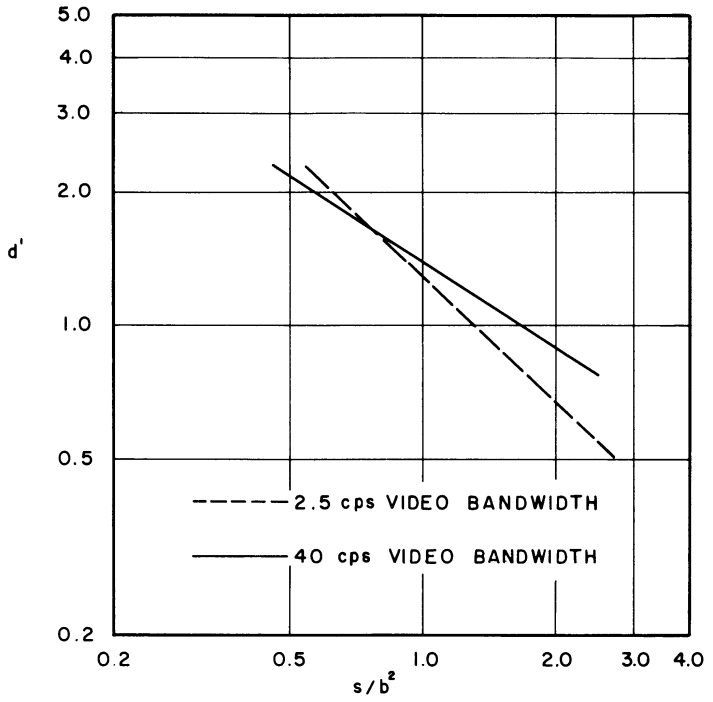

FIG. 17 d' vs. NORMALIZED SWEEP SPEED, $\frac{s}{b^2}$

LINEAR DETECTOR
S/N = 10.7
T_o = 0.5 SEC

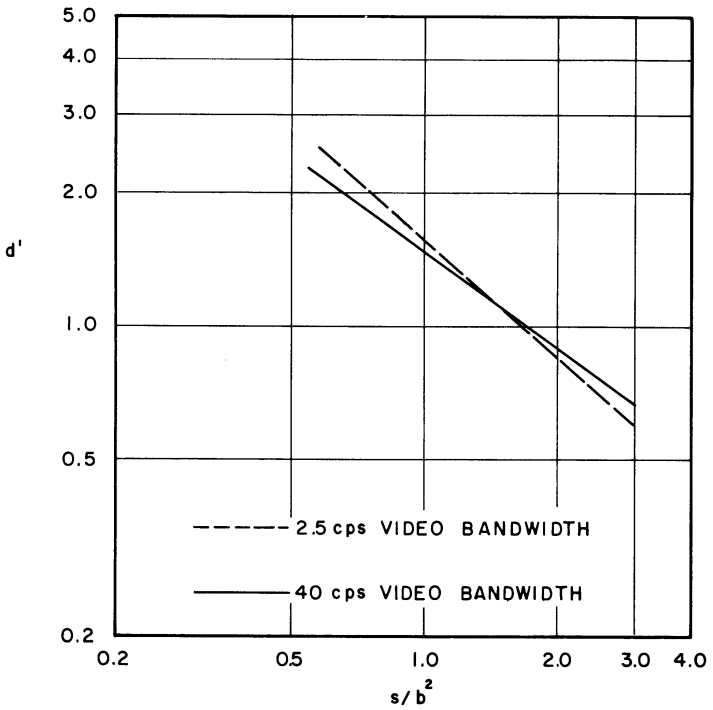

FIG. 18 d' vs. NORMALIZED SWEEP SPEED, $\frac{s}{b^2}$

SQUARE LAW DETECTOR
S/N = 10.7
T_o = 0.5 SEC.

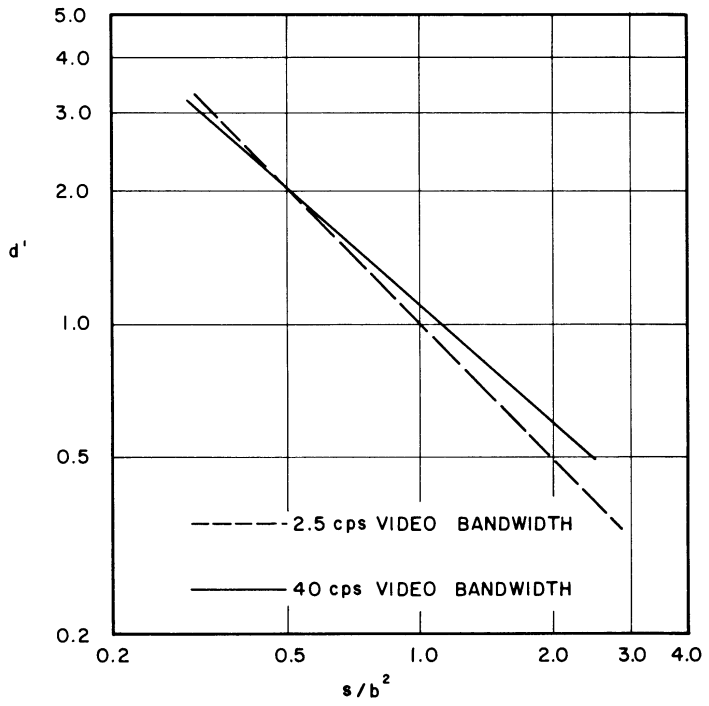

FIG. 19 d' vs. NORMALIZED SWEEP SPEED, $\frac{s}{b^2}$

LINEAR DETECTOR
S/N = 10.7
T_o = 1.2 SEC

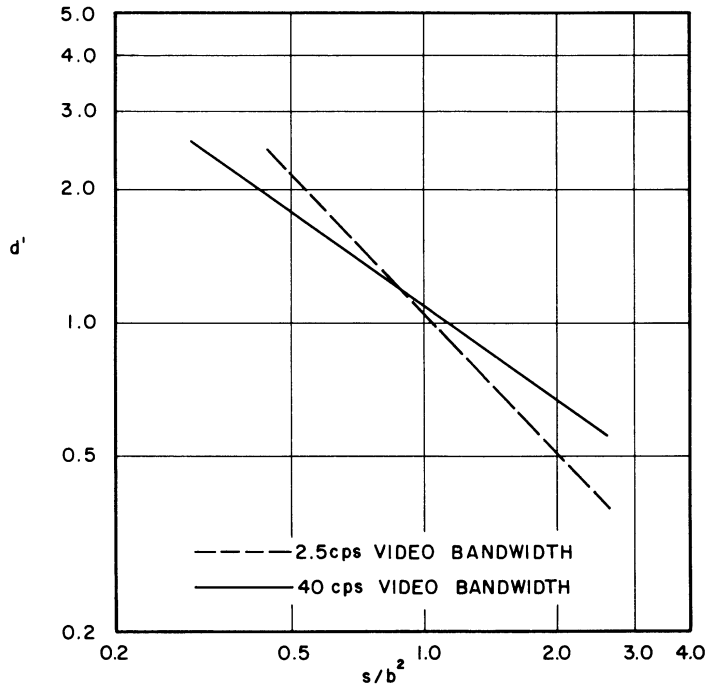

FIG. 20 d' vs NORMALIZED SWEEP SPEED, $\frac{s}{b^2}$

SQUARE LAW DETECTOR
S/N =10.7
T_o = 1.2 SEC

interval. Furthermore, for the same observation time interval, it is lower for the linear detector than for the square law detector. Recall that Figure 13 shows the crossover point for the linear detector as a function of T_o.

It will be seen shortly that any choice of video bandwidth for best signal detection must be either the wide or narrow bandwidth. From the foregoing discussion, the selection of wide or narrow bandwidth will depend upon the region in the $\frac{s}{b^2} - T_o$ plane in which the receiver is operating.

In Figures 17 through 20, the square law detector yields generally better signal detection than the linear detector. The variation of d' as a function of sweep speed can be expressed approximately as

$$d' \propto \left(\frac{s}{b^2}\right)^{-1} \tag{4}$$

for the narrow video bandwidth, and

$$d' \propto \left(\frac{s}{b^2}\right)^{-\frac{1}{2}} \tag{5}$$

for the wide video bandwidth. These approximate relationships hold for both detector cases and are independent of time interval and signal-to-noise ratio.

4.2.4 d' as a Function of Video Bandwidth, β

In order to determine the video filter bandwidth which yields best signal detection, d' values were obtained for the several video bandwidths available, at different sweep speeds. Figures 21, 22, and 23 present the results.

The trend reported previously is substantiated in these figures.

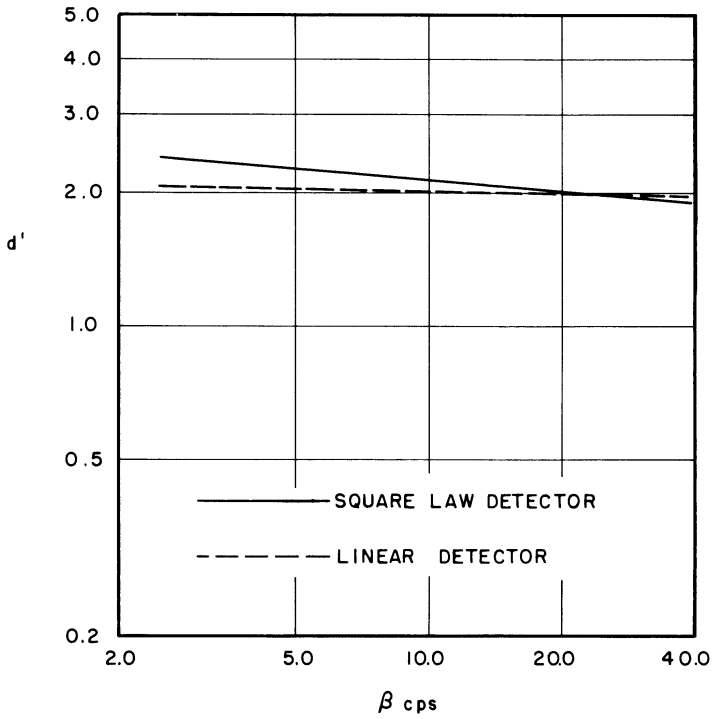

FIG. 21 d' vs VIDEO BANDWIDTH, β

S/N = 10.7 , T_o = 0.5 SEC

s/b^2 = 0.6

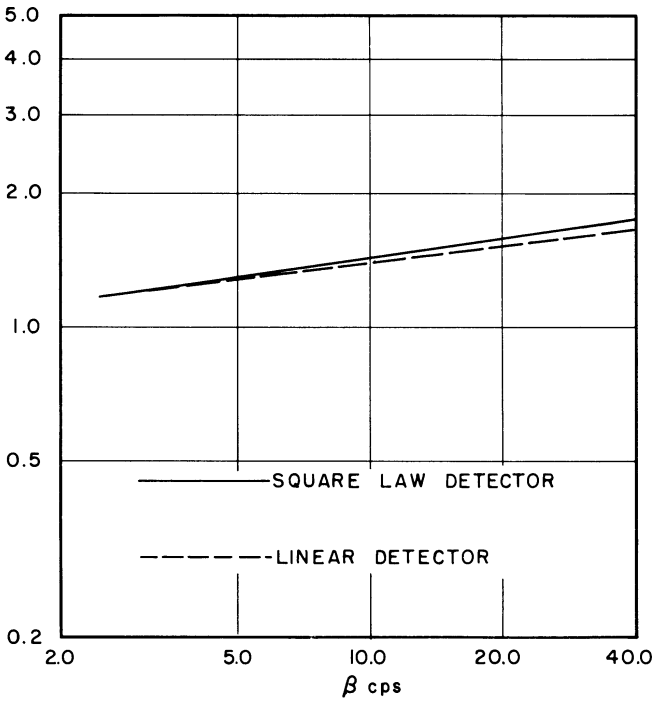

FIG. 22 d' vs. VIDEO BANDWIDTH, β

S/N = 24.5 , T_o = 0.5 SEC

s/b^2 = 2.5

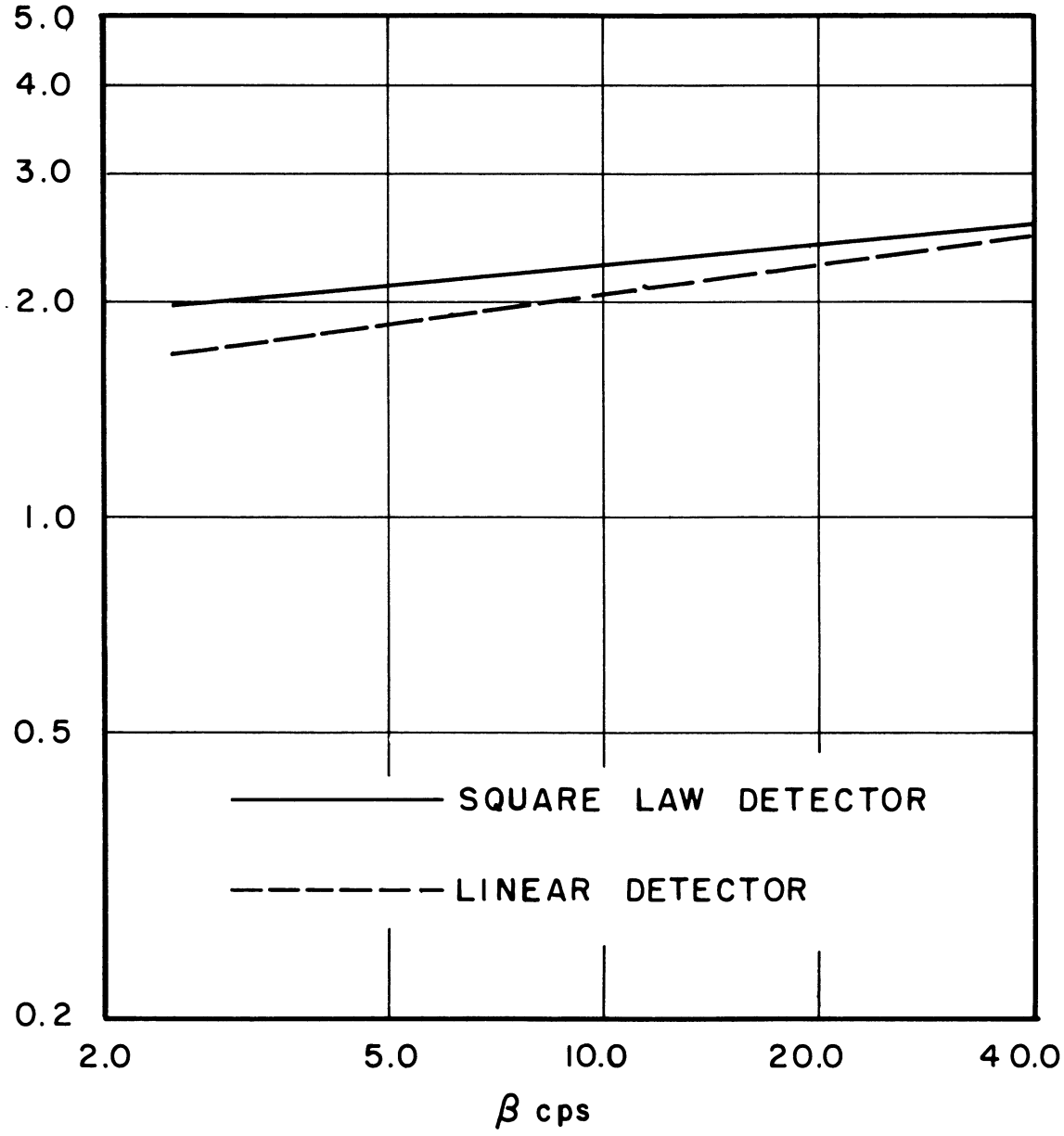

FIG. 23 d' vs. VIDEO BANDWIDTH, β

S/N = 18 , T = 0.8 SEC.

$s/b^2 = 1.1$

That is, at low sweep speeds the narrow video bandwidth yields better detection, while at high sweep speeds the wide video bandwidth is better. But, it is also apparent that no optimum video bandwidth exists at any sweep speed which is not either very wide (essentially no filtering) or very narrow (integrator-like). Figure 24, which represents a three-dimensional map of d' against sweep speed and video bandwidth for a system with constant S/N and T_o, emphasizes this point. The map is a plane surface which is twisted for increasing sweep speed.

Figures 13, 17, 18, 19, and 20 have been used to roughly obtain the division in the $\frac{s}{b^2} - T_o$ plane between the wide and narrow filters. The separatrices for the two detector cases are shown in Figure 25.

5. FORMULATION OF THE EXPERIMENTAL RESULTS

The experimental data presented in this report can be represented in an approximate formulation utilizing Eqs. (2) through (5). For the narrow video bandwidth,

$$d' \propto \frac{\left(\frac{S}{N}\right)}{(bT_o)^{\frac{1}{3}} \left(\frac{s}{b^2}\right)} \tag{6}$$

By squaring (6) an effective output signal-to-noise ratio is obtained.

$$\left(\frac{S}{N}\right)_{out} \propto \frac{\left(\frac{S}{N}\right)^2}{(bT_o)^{\frac{2}{3}} \left(\frac{s}{b^2}\right)^2} \tag{7}$$

Now, making use of the following,

$$N = N_o b \tag{8}$$

$$B = sT_o , \tag{9}$$

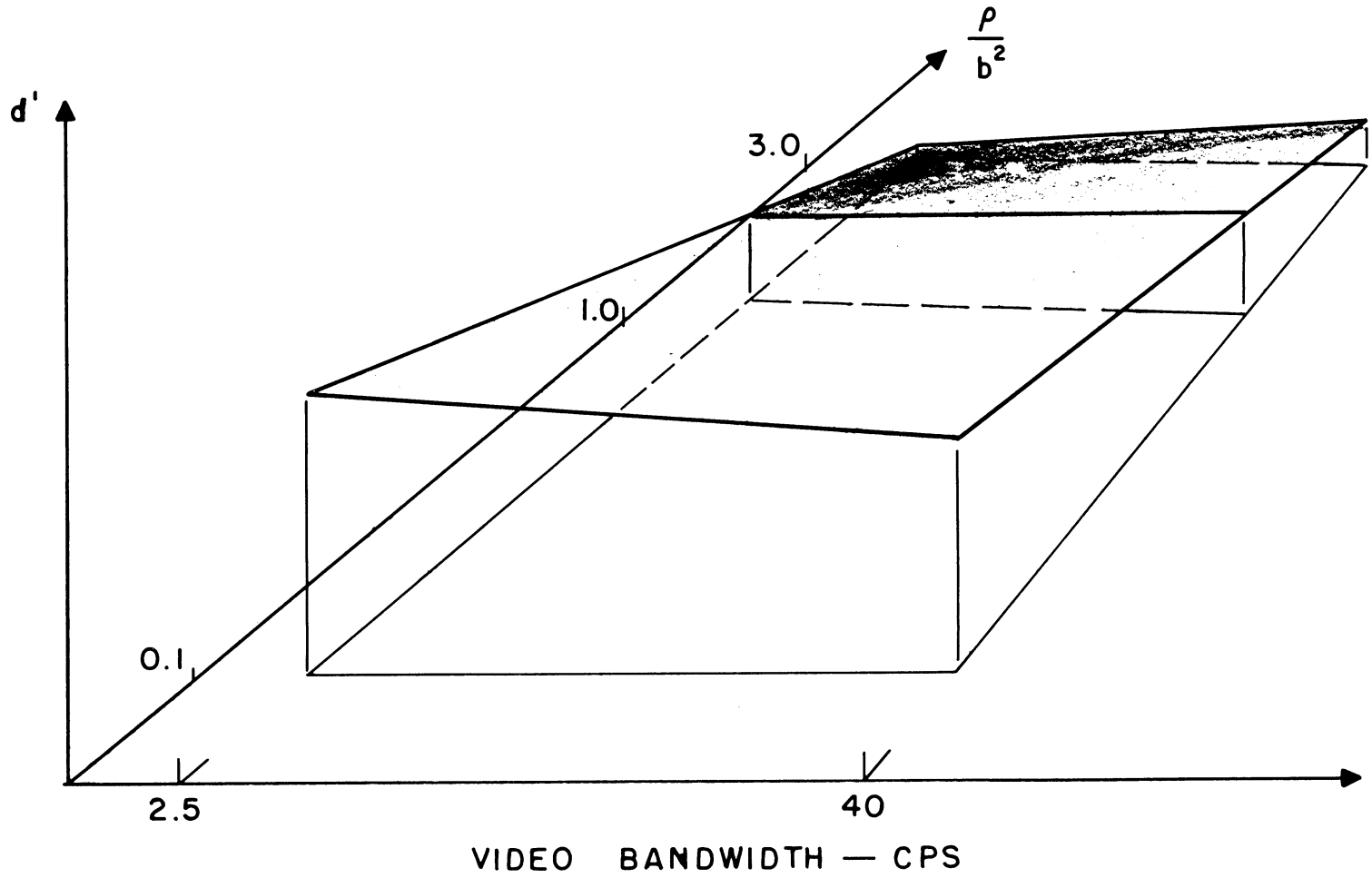

FIG. 24 SURFACE OF d' AGAINST SWEEP SPEED AND VIDEO BANDWIDTH

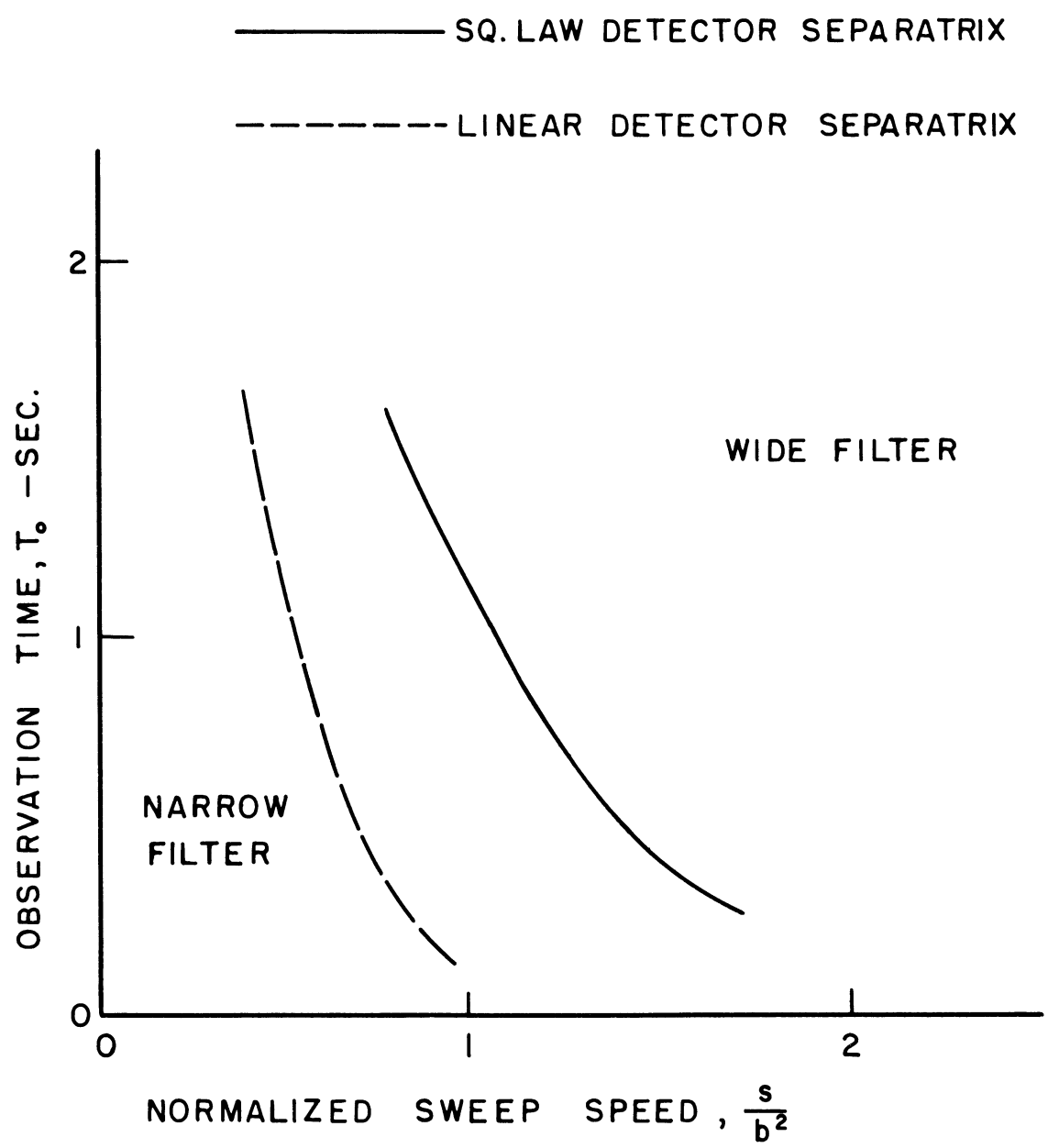

FIG. 25 OPTIMUM VIDEO FILTER BANDWIDTH IN $\frac{s}{b^2} - T_o$ PLANE

where N_o = noise power/unit bandwidth, B = frequency band swept by the receiver (rad./sec), Eq. (7) can be written as

$$\left(\frac{S}{N}\right)_{out} \propto \frac{S^2}{N_o^2} \frac{b^2 T_o^2}{(bT_o)^{\frac{2}{3}} (B^2)}$$

or

$$\left(\frac{S}{N}\right)_{out} \propto \left(\frac{S}{N_B}\right)^2 (bT_o)^{\frac{4}{3}} , \tag{10}$$

where N_B is the noise power in the band swept by the receiver. bT_o in Eq. (9) represents the normalized sweep time. For the wide video bandwidth,

$$d' \propto \frac{\left(\frac{S}{N}\right)}{(bT_o)^{\frac{1}{3}} \left(\frac{s}{b^2}\right)^{\frac{1}{2}}} , \tag{11}$$

and

$$\left(\frac{S}{N}\right)_{out} \propto \frac{S}{N} \cdot \frac{S}{N_B} \cdot (bT_o)^{\frac{1}{3}} . \tag{12}$$

Although Eqs. (10) and (12) may appear to indicate that the effective output signal-to-noise ratio is independent of sweep speed, such is not the case. Consider a fixed band swept. As T_o is increased, $\left(\frac{S}{N}\right)_{out}$ also increases. But the sweep speed must decrease to hold the band swept constant, so the $\left(\frac{S}{N}\right)_{out}$ would be expected to increase.

6. SUMMARY

The effects of sweep speed, sweep time, input signal-to-noise ratio, and video filter bandwidth on detection of a continuous signal by

a panoramic receiver have been described. It has been shown that a square law detector characteristic yields slightly better signal detection than the linear detector in general.

Furthermore, it has been shown that the only existing choices of video filter bandwidth to yield best signal detection are a very narrow or a very wide bandwidth. Which of these two yields the best detection depends upon the sweep speed and sweep time of the receiver.

APPENDICES

The data obtained in these experiments are tabulated here for the benefit of the reader. Probabilities are given as percentages. These are estimates obtained from the SIMRAR counters. For each set of signal and receiver parameters the threshold circuits of Fig. 1 are adjusted to give a reasonable range of values for the estimated false alarm probability. The false alarm probability estimate $P_N(A)$ for each channel is the number of times the voltage exceeds the channel's threshold level divided by the number of trials with noise alone. Similarly, the detection probability estimate $P_{SN}(A)$ is the number of times the signal-plus-noise output voltage exceeds the channel's threshold divided by the number of trials with signal plus noise. These numbers, multiplied by one hundred, are the entries in the tables which follow.

When these data are plotted on double probability paper, as illustrated in Figs. 7-11, the 45 degree line best fitting the data gives a measure of the detectibility index d'.[1]

The number of trials taken on each alternative is indicated in this tabulation.

---

[1] Section 3.

APPENDIX A

SQUARE LAW DETECTOR

TABLE A-I

Variable S/N, T_o = 0.5 sec, s/b^2 = 0.6, β = 2.5 cps

(a) S/N = 10.7, d' = 2.44, 500 trials									
$P_{SN}(A)$	98.6	97.8	97.0	95.2	92.8	91.0	89.6	82.2	78.4
$P_N(A)$	55.0	38.6	32.2	24.6	17.2	13.4	11.2	6.4	4.2
(b) S/N = 7.8, d' = 1.56, 1000 trials									
$P_{SN}(A)$	98.1	92.5	90.5	94.3	85.8	81.9	78.4	67.0	59.5
$P_N(A)$	72.1	48.4	43.0	54.2	32.6	25.8	22.3	10.4	7.7
(c) S/N = 5.3, d' = 1.18, 500 trials									
$P_{SN}(A)$	97.0	92.2	91.2	91.4	80.8	73.4	65.2	48.0	43.4
$P_N(A)$	83.2	67.4	63.4	64.8	40.2	26.0	19.4	9.0	7.4
(d) S/N = 3.85, d' = 0.77, 500 trials									
$P_{SN}(A)$	91.6	78.8	77.0	77.4	65.6	60.0	58.0	40.6	35.8
$P_N(A)$	67.6	53.4	50.2	52.4	35.6	29.4	26.4	13.8	10.2

TABLE A-II

Variable S/N, T_o = 0.5 sec, s/b^2 = 0.6, β = 40 cps

(a) S/N = 10.7, d' = 2.12, 500 trials									
$P_{SN}(A)$	93.2	89.0	88.6	88.8	87.4	84.0	83.2	80.2	77.0
$P_N(A)$	31.0	22.2	19.2	19.4	16.0	13.0	11.8	9.8	8.0
(b) S/N = 7.8, d' = 1.38, 500 trials									
$P_{SN}(A)$	87.8	83.4	82.0	82.6	77.8	75.6	74.2	68.8	65.2
$P_N(A)$	51.0	38.8	35.0	35.8	26.2	22.0	20.8	16.4	14.8
(c) S/N = 5.3, d' = 0.92, 500 trials									
$P_{SN}(A)$	89.4	84.4	82.2	82.8	77.2	73.4	71.2	65.4	61.2
$P_N(A)$	66.6	56.6	52.4	53.2	44.0	39.2	37.6	29.2	26.2
(d) S/N = 3.85, d' = 0.70, 500 trials									
$P_{SN}(A)$	86.4	79.4	77.2	71.6	66.2	62.6	62.0	56.0	52.4
$P_N(A)$	69.0	56.4	52.8	47.4	40.8	36.4	35.0	27.4	22.2

TABLE A-III

Variable S/N, T_o = 0.5 sec, s/b^2 = 2.5, β = 2.5 cps

(a) S/N = 10.7, d' = 0.70, 500 trials									
$P_{SN}(A)$	78.2	69.4	64.6	56.6	45.2	39.4	42.8	30.6	30.6
$P_N(A)$	52.6	43.6	37.2	29.0	20.6	17.8	20.0	12.6	12.2
(b) S/N = 15.3, d' = 1.0, 500 trials									
$P_{SN}(A)$	89.0	85.0	81.4	77.4	70.6	65.8	63.8	53.6	46.4
$P_N(A)$	57.4	50.6	45.8	41.6	34.0	27.4	25.8	17.6	13.6
(c) S/N = 19, d' = 1.20, 500 trials									
$P_{SN}(A)$	95.6	88.4	85.0	85.2	78.4	73.6	71.0	56.4	50.0
$P_N(A)$	69.0	49.0	44.0	44.4	34.8	28.2	24.8	16.6	12.4
(d) S/N = 24.5, d' = 1.52, 500 trials									
$P_{SN}(A)$	96.0	90.6	87.4	84.2	83.6	81.0	78.4	68.0	59.8
$P_N(A)$	62.8	44.8	39.4	34.4	31.8	24.8	21.6	13.6	9.4

TABLE A-IV

Variable S/N, T_o = 0.5 sec, s/b^2 = 2.5, β = 40 cps

(a) S/N = 10.7, d' = .76, 500 trials									
$P_{SN}(A)$	82.8	76.0	72.2	68.2	63.2	60.2	57.8	49.6	46.0
$P_N(A)$	60.6	48.4	44.6	39.4	32.8	29.0	28.0	20.8	16.8
(b) S/N = 15.3, d' = 1.38, 500 trials									
$P_{SN}(A)$	92.4	89.6	88.2	85.8	82.2	79.8	78.2	73.0	67.4
$P_N(A)$	62.0	49.8	45.2	39.2	33.6	29.6	27.4	21.8	19.2
(c) S/N = 19, d' = 1.56, 500 trials									
$P_{SN}(A)$	87.0	81.4	79.6	76.4	71.4	68.4	67.0	62.4	58.8
$P_N(A)$	36.0	27.2	23.4	19.4	15.8	12.2	11.0	8.0	6.4
(d) S/N = 24.5, d' = 1.98, 500 trials									
$P_{SN}(A)$	94.4	89.8	88.8	87.2	82.8	80.4	78.8	74.8	72.0
$P_N(A)$	39.8	29.0	24.8	20.6	16.6	12.6	11.6	8.4	5.2

TABLE A-V

Variable s/b^2, T_o = 0.5 sec, S/N = 10.7, β = 2.5 cps

(a) s/b^2 = 1.1, d' = 1.58, 500 trials									
$P_{SN}(A)$	89.2	82.6	78.4	73.8	67.2	57.6	47.8	43.4	38.2
$P_N(A)$	37.8	26.8	22.8	19.4	12.4	8.0	4.6	2.8	1.8
(b) s/b^2 = 1.8, d' = 0.98, 500 trials									
$P_{SN}(A)$	94.4	88.0	85.4	83.0	77.4	71.8	66.2	51.2	39.8
$P_N(A)$	74.2	57.8	53.6	49.2	41.4	36.4	28.2	16.0	9.6

TABLE A-VI

Variable s/b^2, T_o = 0.5 sec, S/N = 10.7, β = 40 cps

(a) s/b^2 = 1.1, d' = 1.37, 500 trials								
$P_{SN}(A)$	95.4	92.2	88.2	84.0	80.2	75.4	59.4	53.0
$P_N(A)$	68.6	59.0	48.4	38.8	33.8	25.4	9.8	6.6
(b) s/b^2 = 1.8, d' = 0.96, 500 trials								
$P_{SN}(A)$	86.0	79.8	74.6	74.8	62.0	55.4	39.6	34.0
$P_N(A)$	62.0	50.2	39.4	40.0	25.8	17.6	7.0	4.8

TABLE A-VII

Variable s/b^2, T_o = 1.2 sec, S/N = 10.7, β = 2.5 cps

(a) s/b^2 = 1.1, d' = 1.0, 500 trials									
$P_{SN}(A)$	94.6	90.4	87.8	85.2	78.4	75.0	73.6	65.6	60.8
$P_N(A)$	80.6	65.8	60.0	56.8	47.2	41.2	38.6	27.8	22.4
(b) s/b^2 = 1.8, d' = 0.55, 500 trials									
$P_{SN}(A)$	91.6	83.6	80.8	77.4	68.6	63.8	59.4	47.4	42.6
$P_N(A)$	81.2	68.6	64.6	59.6	48.8	42.6	40.0	26.4	20.2
(c) s/b^2 = 2.5, d' = 0.40, 500 trials									
$P_{SN}(A)$	87.0	75.3	68.9	65.5	57.1	52.9	48.7	36.4	31.2
$P_N(A)$	78.8	63.7	57.3	52.6	41.9	34.2	32.0	20.4	17.2

TABLE A-VIII

Variable s/b^2, T_o = 1.2 sec, S/N = 10.7, β = 40 cps

(a) s/b^2 = 0.3, d' = 2.55, 1000 trials								
$P_{SN}(A)$	98.9	98.7	98.0	96.8	96.0	94.9	94.7	
$P_N(A)$	44.4	40.2	37.5	26.0	22.1	18.5	18.0	
(b) s/b^2 = 1.1, d' = 1.09, 1000 trials								
$P_{SN}(A)$	84.5	77.7	75.2	73.0	65.8	62.4	58.3	57.6
$P_N(A)$	51.1	39.5	36.4	33.3	24.8	21.0	16.6	15.9
(c) s/b^2 = 2.5, d' = 0.56, 500 trials								
$P_{SN}(A)$	79.4	69.0	64.4	62.0	55.2	51.8	48.4	41.2	37.6
$P_N(A)$	61.0	49.2	43.8	38.8	32.6	29.4	27.4	21.6	17.0

TABLE A-IX

Variable T_o, s/b^2 = 2.5, S/N = 24.5, β = 2.5 cps

(a) T_o = 0.8, d' = 1.20, 500 trials									
$P_{SN}(A)$	79.6	70.2	66.6	65.2	59.0	52.8	49.6	40.8	36.2
$P_N(A)$	38.6	24.6	20.6	19.2	13.8	11.6	9.6	7.2	5.6
(b) T_o = 1.6, d' = 1.02, 500 trials									
$P_{SN}(A)$	91.2	83.6	80.8	79.2	73.4	66.4	64.0	53.6	49.8
$P_N(A)$	67.2	52.4	45.8	42.6	35.4	27.8	25.2	15.4	10.6
(c) T_o = 3.2, d' = 0.80, 500 trials									
$P_{SN}(A)$	97.0	90.6	87.4	86.0	78.8	74.8	72.0	59.6	52.4
$P_N(A)$	86.8	73.4	67.2	64.8	53.8	45.0	42.4	28.6	23.0

TABLE A-X

Variable T_o, $s/b^2 = 2.5$, $S/N = 24.5$, $\beta = 40$ cps

(a) $T_o = 0.8$, $d' = 1.84$, 500 trials									
$P_{SN}(A)$	91.6	88.8	87.6	86.4	84.2	83.0	81.4	78.2	76.2
$P_N(A)$	41.8	31.0	28.4	25.2	21.0	18.6	16.8	13.2	11.2
(b) $T_o = 1.6$, $d' = 1.52$, 500 trials									
$P_{SN}(A)$	95.8	92.4	91.2	90.6	89.0	86.6	84.6	80.2	76.2
$P_N(A)$	64.6	52.0	48.2	45.2	39.4	33.6	31.6	26.8	22.4
(c) $T_o = 3.2$, $d' = 1.12$, 500 trials									
$P_{SN}(A)$	98.6	96.4	93.1	92.1	90.7	89.5	88.2	83.3	78.9
$P_N(A)$	89.0	77.2	72.5	69.3	63.1	57.9	54.0	44.7	38.9

TABLE A-XI

Variable T_o, $s/b^2 = 0.6$, $S/N = 10.7$, $\beta = 2.5$ cps

(a) $T_o = 0.8$, $d' = 2.10$, 500 trials									
$P_{SN}(A)$	98.0	95.2	94.6	93.2	90.4	88.4	86.0	79.2	74.2
$P_N(A)$	62.6	42.4	36.8	32.2	23.8	18.2	17.0	8.8	6.0
(b) $T_o = 1.6$, $d' = 1.90$, 500 trials									
$P_{SN}(A)$	99.4	97.8	97.4	96.4	95.0	92.4	91.0	86.2	80.8
$P_N(A)$	88.0	69.2	61.4	54.4	43.2	35.6	32.8	19.4	15.4
(c) $T_o = 3.2$, $d' = 1.6$, 1000 trials									
$P_{SN}(A)$	99.9	97.6	96.8	95.5	90.8	87.7	86.2	77.7	71.1
$P_N(A)$	92.9	76.6	68.0	57.8	45.0	35.4	31.5	20.3	13.3

TABLE A-XII

Variable T_o, $s/b^2 = 0.6$, $S/N = 10.7$, $\beta = 40$ cps

(a) $T_o = 0.8$, d' = 1.76, 500 trials									
$P_{SN}(A)$	96.0	91.2	90.6	87.6	84.8	82.4	81.4	76.0	72.2
$P_N(A)$	52.2	39.2	35.6	30.2	24.4	20.6	18.2	12.8	10.8
(b) $T_o = 1.0$, d' = 1.66, 1000 trials									
$P_{SN}(A)$	90.7	86.7	84.9	83.1	79.1	76.6	73.0	72.7	
$P_N(A)$	42.9	31.8	29.0	25.4	17.9	15.9	12.4	12.0	
(c) $T_o = 2.0$, d' = 1.30, 500 trials									
$P_{SN}(A)$	92.8	88.4	86.8	84.8	78.8	76.4	71.4	70.6	
$P_N(A)$	63.6	51.0	46.0	43.0	33.4	28.8	23.0	22.6	

TABLE A-XIII

Variable β, $T_o = 0.5$ sec, $S/N = 10.7$, $s/b^2 = 0.6$

(a) $\beta = 5$ cps, d' = 2.25, 500 trials								
$P_{SN}(A)$	96.0	92.4	91.2	88.8	80.2	75.0	68.2	62.6
$P_N(A)$	36.2	21.6	19.6	14.8	8.0	5.6	3.8	2.2
(b) $\beta = 10$ cps, d' = 2.10, 500 trials								
$P_{SN}(A)$	88.4	84.8	82.8	79.6	71.8	65.4		
$P_N(A)$	17.8	12.4	11.6	10.0	5.0	3.8		
(c) $\beta = 20$ cps, d' = 2.09, 500 trials								
$P_{SN}(A)$	92.0	86.4	85.4	83.4	77.2	73.4		
$P_N(A)$	27.6	19.0	17.4	13.8	8.2	5.2		
(d) $\beta = 40$ cps, d' = 1.96, 500 trials								
$P_{SN}(A)$	85.6	79.0	76.8	74.2	66.8			
$P_N(A)$	18.4	11.4	10.2	7.8	4.0			

TABLE A-XIV

Variable β, T_o = 0.5 sec, S/N = 24.5, s/b^2 = 2.5

(a) β = 2.5 cps, d' = 1.2, 1000 trials								
$P_{SN}(A)$	93.4	86.9	80.2	81.7	64.7	51.3	25.3	18.8
$P_N(A)$	66.3	48.1	36.6	38.3	18.4	10.6	2.5	1.5
(b) β = 5 cps, d' = 1.32, 500 trials								
$P_{SN}(A)$	95.6	93.8	87.8	90.2	70.4	62.0	47.8	38.0
$P_N(A)$	66.6	60.0	45.4	47.4	22.2	15.0	7.6	4.0
(c) β = 10 cps, d' = 1.5, 500 trials								
$P_{SN}(A)$	96.2	94.4	90.6	91.2	82.6	77.0	55.2	48.6
$P_N(A)$	70.4	57.2	46.0	46.8	32.2	22.4	8.0	4.2
(d) β = 20 cps, d' = 1.52, 500 trials								
$P_{SN}(A)$	92.4	90.8	84.4	85.0	68.0	62.4	52.8	45.0
$P_N(A)$	48.8	42.2	32.2	33.0	14.0	11.2	5.8	3.4
(e) β = 40 cps, d' = 1.76, 500 trials								
$P_{SN}(A)$	95.6	94.0	90.8	84.0	80.8	67.8	63.2	
$P_N(A)$	55.4	43.2	36.4	23.4	17.6	9.6	5.6	

TABLE A-XV

Variable β, T_o = 0.8 sec, S/N = 18, s/b^2 = 1.1

(a) β = 2.5 cps, d' = 2.08, 1000 trials									
$P_{SN}(A)$	98.2	94.5	92.4	91.0	83.2	78.2	36.2	68.2	65.1
$P_N(A)$	51.0	31.6	26.7	22.4	13.2	9.7	1.1	4.7	3.6
(b) β = 5 cps, d' = 2.09, 1000 trials									
$P_{SN}(A)$	96.9	91.6	89.5	88.2	81.6	78.5	45.6	70.6	66.4
$P_N(A)$	39.4	25.9	21.6	18.8	10.4	7.9	1.7	5.1	4.2
(c) β = 20 cps, d' = 2.25, 1000 trials									
$P_{SN}(A)$	96.8	95.0	94.4	93.9	92.6	88.3	89.9	89.0	
$P_N(A)$	44.6	34.6	31.8	27.3	24.0	14.1	18.0	15.5	
(d) β = 40 cps, d' = 2.52, 500 trials									
$P_{SN}(A)$	97.6	96.4	96.0	95.2	95.2	95.0	90.8	92.8	92.4
$P_N(A)$	45.2	35.0	32.2	29.8	28.6	24.2	12.2	16.0	13.0

APPENDIX B

LINEAR DETECTOR

TABLE B-I

Variable S/N, T_o = 0.5 sec, s/b^2 = 0.6, β = 2.5 cps

(a) S/N = 10.7, d' = 2.06, 500 trials									
$P_{SN}(A)$	98.4	92.4	87.4	84.0	74.4	66.6	61.2	41.6	32.0
$P_N(A)$	47.6	24.2	19.2	15.6	10.6	6.4	4.8	1.8	1.0
(b) S/N = 7.8, d' = 1.42, 500 trials									
$P_{SN}(A)$	94.4	82.8	77.0	73.8	63.6	54.0	59.0	40.6	40.2
$P_N(A)$	55.4	31.4	25.4	21.8	14.8	11.2	13.0	5.2	4.6
(c) S/N = 5.3, d' = 0.98, 500 trials									
$P_{SN}(A)$	92.8	80.4	75.6	73.4	58.4	49.6	52.8	35.8	35.0
$P_N(A)$	66.0	44.0	37.4	34.8	23.8	19.0	20.6	11.0	10.8
(d) S/N = 3.85, d' = 0.70, 500 trials									
$P_{SN}(A)$	79.8	58.0	51.0	48.2	35.4	28.0	32.2	16.8	16.0
$P_N(A)$	54.6	29.6	25.0	20.8	12.0	8.2	10.0	4.4	4.4

TABLE B-II

Variable S/N, T_o = 0.5 sec, s/b^2 = 0.6, β = 40 cps

(a) S/N = 10.7, d' = 1.96, 500 trials									
$P_{SN}(A)$	99.2	97.2	96.0	96.4	92.8	90.6	87.8	79.0	72.6
$P_N(A)$	82.4	57.6	50.0	50.8	38.6	28.4	24.4	14.2	6.6
(b) S/N = 7.8, d' = 1.62, 500 trials									
$P_{SN}(A)$	98.6	94.4	91.2	88.0	82.0	75.2	71.6	57.6	49.2
$P_N(A)$	70.6	48.8	44.2	33.2	22.8	15.6	13.6	8.4	5.4
(c) S/N = 5.3, d' = 1.0, 500 trials									
$P_{SN}(A)$	94.8	86.0	84.0	79.2	71.8	64.4	61.2	49.4	40.4
$P_N(A)$	83.8	60.6	54.8	45.2	35.2	24.4	22.0	12.8	9.0
(d) S/N = 3.85, d' = 0.70, 500 trials									
$P_{SN}(A)$	95.2	83.6	79.2	73.8	62.6	54.4	48.2	31.6	22.8
$P_N(A)$	84.6	64.8	58.4	47.2	34.2	26.8	23.6	13.0	6.4

TABLE B-III

Variable S/N, $T_o = 0.5$, $s/b^2 = 2.5$, $\beta = 2.5$ cps

(a) S/N = 10.7, d' = 0.76, 500 trials									
$P_{SN}(A)$	76.4	64.0	62.0	65.8	55.6	52.0	52.2	36.8	29.4
$P_N(A)$	54.4	34.6	31.4	36.0	26.2	22.8	22.8	12.4	9.8
(b) S/N = 15.3, d' = 1.0, 500 trials									
$P_{SN}(A)$	93.0	87.8	88.8	86.0	80.2	72.4	77.0	56.0	54.8
$P_N(A)$	69.4	58.0	58.8	54.8	43.4	35.4	40.0	22.6	22.0
(c) S/N = 19, d' = 1.12, 1000 trials									
$P_{SN}(A)$	79.0	69.3	60.9	74.2	63.7	63.7	59.0	48.7	47.3
$P_N(A)$	37.1	26.7	20.2	31.6	22.5	22.4	19.2	11.9	11.4
(d) S/N = 24.5, d' = 1.30, 1000 trials									
$P_{SN}(A)$	89.4	80.8	82.1	85.6	75.4	66.1	70.6	52.6	52.1
$P_N(A)$	46.2	33.9	35.6	40.8	28.0	20.7	23.8	10.2	9.7

TABLE B-IV

Variable S/N, $T_o = 0.5$, $s/b^2 = 2.5$, $\beta = 40$ cps

(a) S/N = 10.7, d' = 0.64, 1000 trials									
$P_{SN}(A)$	77.0	68.5	70.3	73.2	64.9	58.9	61.8	49.6	47.9
$P_N(A)$	53.5	43.8	45.2	49.1	39.2	34.1	35.8	26.0	24.2
(b) S/N = 15.3, d' = 1.08, 1000 trials									
$P_{SN}(A)$	75.8	70.0	71.8	72.7	66.5	63.3	64.3	54.7	53.1
$P_N(A)$	38.3	29.8	31.3	33.7	25.5	20.7	22.8	14.0	13.2
(c) S/N = 19, d' = 1.28, 1000 trials									
$P_{SN}(A)$	84.4	79.2	80.1	81.6	76.7	73.1	74.0	65.8	64.7
$P_N(A)$	43.5	35.1	37.2	39.6	30.2	24.4	27.6	16.5	15.4
(d) S/N = 24.5, d' = 1.83, 1000 trials									
$P_{SN}(A)$	84.9	81.0	81.1	81.6	78.0	73.7	75.3	66.9	66.1
$P_N(A)$	23.3	16.1	16.8	17.0	12.9	10.1	11.5	6.6	6.3

TABLE B-V

Variable s/b^2, $T_o = 0.5$, $S/N = 10.7$, $\beta = 2.5$ cps

(a) $s/b^2 = 1.1$, $d' = 1.16$, 1000 trials									
$P_{SN}(A)$	87.1	78.7	79.6	82.1	73.0	64.6	70.4	49.8	50.2
$P_N(A)$	48.0	36.6	38.3	43.5	28.9	22.0	26.0	11.8	11.9
(b) $s/b^2 = 1.8$, $d' = 0.74$, 1000 trials									
$P_{SN}(A)$	81.9	72.0	73.0	76.5	65.7	59.0	62.4	42.2	42.6
$P_N(A)$	59.1	45.4	46.8	52.7	37.6	28.7	33.3	17.8	17.9

TABLE B-VI

Variable s/b^2, $T_o = 0.5$, $S/N = 10.7$, $\beta = 40$ cps

(a) $s/b^2 = 0.3$, $d' = 3.0$, 500 trials								
$P_{SN}(A)$	97.6	95.0	93.2	92.6	85.8	83.0		
$P_N(A)$	19.4	9.0	7.0	5.6	3.2	1.4		
(b) $s/b^2 = 1.1$, $d' = 1.47$, 500 trials								
$P_{SN}(A)$	97.2	92.6	91.0	89.2	81.6	76.8	69.6	69.4
$P_N(A)$	77.0	57.8	50.2	45.2	27.2	22.4	17.0	16.6
(c) $s/b^2 = 1.8$, $d' = 1.0$, 500 trials								
$P_{SN}(A)$	94.4	88.2	84.2	81.4	70.4	66.0	55.2	55.0
$P_N(A)$	81.6	65.6	55.2	49.4	31.8	26.0	19.0	18.6

TABLE B-VII

Variable s/b^2, $T_o = 1.2$, $S/N = 10.7$, $\beta = 2.5$ cps

(a) $s/b^2 = 0.3$, $d' = 3.4$, 1000 trials								
$P_{SN}(A)$	98.8	97.5	95.1	95.3				
$P_N(A)$	12.9	7.2	4.1	4.3				
(b) $s/b^2 = 1.1$, $d' = 0.97$, 1000 trials								
$P_{SN}(A)$	96.2	84.3	77.5	71.9	44.1	31.8	20.9	22.4
$P_N(A)$	80.6	51.0	40.5	34.8	13.8	8.0	4.3	4.4
(c) $s/b^2 = 1.8$, $d' = 0.55$, 1000 trials								
$P_{SN}(A)$	92.9	77.5	68.1	62.7	36.8	24.0	14.1	14.4
$P_N(A)$	84.5	56.8	47.0	41.2	16.3	10.5	5.2	5.4
(d) $s/b^2 = 2.5$, $d' = 0.36$, 1000 trials								
$P_{SN}(A)$	91.0	74.0	64.3	56.9	29.1	18.8	9.6	10.2
$P_N(A)$	85.2	58.9	48.7	42.3	19.5	10.9	4.9	5.0

TABLE B-VIII

Variable s/b^2, $T_o = 1.2$, $S/N = 10.7$, $\beta = 40$ cps

(a) $s/b^2 = 1.1$, $d' = 1.1$, 1000 trials								
$P_{SN}(A)$	95.3	88.0	82.9	79.5	65.6	59.0	48.8	48.6
$P_N(A)$	77.5	57.9	50.7	45.1	23.7	17.8	10.2	10.1
(b) $s/b^2 = 1.8$, $d' = 0.70$, 500 trials								
$P_{SN}(A)$	92.0	77.8	69.8	65.6	46.4	40.4	29.0	29.2
$P_N(A)$	74.4	52.8	45.4	40.0	19.8	14.6	9.8	9.6
(c) $s/b^2 = 2.5$, $d' = 0.48$, 1000 trials								
$P_{SN}(A)$	87.6	71.1	64.6	59.3	39.5	33.5	24.5	24.4
$P_N(A)$	78.2	58.0	49.3	42.8	23.0	16.7	10.1	9.9
(d) $s/b^2 = 0.6$, $d' = 1.6$, 1000 trials								
$P_{SN}(A)$	99.0	94.4	91.8	89.7	80.0	75.4	69.1	69.2
$P_N(A)$	79.2	58.9	47.8	41.3	23.3	17.0	11.2	11.0

TABLE B-IX

Variable T_o, $s/b^2 = 2.5$, $S/N = 24.5$, $\beta = 2.5$ cps

(a) $T_o = 0.8$, $d' = 1.22$, 1000 trials									
$P_{SN}(A)$	93.7	88.5	88.9	91.6	83.7	76.9	80.2	62.3	61.6
$P_N(A)$	62.2	48.2	50.6	55.3	40.5	31.9	36.1	18.3	18.1
(b) $T_o = 1.2$, $d' = 1.06$, 1000 trials									
$P_{SN}(A)$	95.3	88.3	88.6	91.7	82.6	74.9	80.2	60.9	59.1
$P_N(A)$	70.5	55.1	56.4	63.3	44.7	34.3	40.7	21.9	20.5
(c) $T_o = 2$, $d' = 0.85$, 1000 trials									
$P_{SN}(A)$	82.1	69.2	70.5	76.2	61.3	52.6	57.9	34.6	33.3
$P_N(A)$	53.3	38.4	39.6	45.6	29.3	19.7	24.8	9.5	9.1

TABLE B-X

Variable T_o, $s/b^2 = 2.5$, $S/N = 24.5$, $\beta = 40$ cps

(a) $T_o = 0.8$, $d' = 1.56$, 1000 trials									
$P_{SN}(A)$	90.1	85.7	86.2	87.5	82.4	78.8	80.3	70.5	69.4
$P_N(A)$	42.9	34.0	35.1	38.4	29.0	21.7	25.0	14.8	13.8
(b) $T_o = 1.2$, $d' = 1.48$, 1000 trials									
$P_{SN}(A)$	89.5	85.4	85.6	86.9	82.9	78.8	80.8	71.6	71.1
$P_N(A)$	49.0	38.9	40.1	43.7	32.5	24.9	27.7	15.5	15.1
(c) $T_o = 2.0$, $d' = 1.24$, 1000 trials									
$P_{SN}(A)$	94.6	91.2	91.8	93.1	88.6	83.9	86.0	76.9	76.1
$P_N(A)$	76.2	64.5	66.5	71.0	55.8	46.2	49.9	32.9	31.4

TABLE B-XI

Variable T_o, $s/b^2 = 0.6$, $S/N = 10.7$, $\beta = 2.5$ cps

(a) $T_o = 0.2$, d' = 2.19, 1000 trials								
$P_{SN}(A)$	99.0	95.7	93.5	91.7	90.1	79.1	65.7	58.4
$P_N(A)$	48.0	28.0	22.4	19.5	17.8	8.0	3.9	3.1
(b) $T_o = 3.0$, d' = 0.88, 500 trials								
$P_{SN}(A)$	99.8	96.2	93.4	88.2	86.4	69.8	52.2	42.4
$P_N(A)$	98.4	86.6	75.8	67.8	64.0	37.8	18.8	13.0
(c) $T_o = 0.3$, d' = 2.07, 1000 trials								
$P_{SN}(A)$	97.8	93.0	91.0	88.2	86.1	75.8	62.5	53.9
$P_N(A)$	45.3	25.7	21.5	18.7	16.2	8.6	4.3	3.2

TABLE B-XII

Variable T_o, $s/b^2 = 0.6$, $S/N = 10.7$, $\beta = 40$ cps

(a) $T_o = 0.2$, d' = 2.25, 1000 trials								
$P_{SN}(A)$	94.9	91.3	89.0	86.7	80.7	77.3	72.7	72.6
$P_N(A)$	28.4	19.4	16.9	13.5	7.0	5.0	3.1	3.1

TABLE B-XIII

Variable β, $s/b^2 = 0.6$, $S/N = 10.7$, $T_o = 0.5$ sec

(a) $\beta = 5$ cps, d' = 1.9, 1000 trials								
$P_{SN}(A)$	97.3	91.2	89.4	87.4	86.3	74.7	65.6	58.3
$P_N(A)$	54.5	32.8	25.1	21.7	18.8	10.4	6.8	4.8
(b) $\beta = 10$ cps, d' = 1.86, 1000 trials								
$P_{SN}(A)$	97.4	94.0	91.9	90.0	89.4	84.4	77.3	72.5
$P_N(A)$	62.2	42.8	35.8	31.5	29.3	19.3	12.5	9.4
(c) $\beta = 20$ cps, d' = 2.02, 1000 trials								
$P_{SN}(A)$	97.9	94.7	93.5	92.3	91.6	87.4	80.1	76.2
$P_N(A)$	60.5	41.2	34.0	29.8	28.1	18.5	10.9	8.6

TABLE B-XIV

Variable β, $s/b^2 = 2.5$, $S/N = 24.5$, $T_o = 0.5$ sec

(a) β = 2.5 cps, d' = 1.06, 500 trials									
$P_{SN}(A)$	96.8	91.2	86.4	84.2	82.4	71.0	36.8	48.4	43.8
$P_N(A)$	80.0	57.0	50.2	46.6	44.2	32.8	8.4	15.0	11.6
(b) β = 10 cps, d' = 1.05, 1000 trials									
$P_{SN}(A)$	95.3	90.7	87.3	85.0	83.8	73.9	62.4	57.0	
$P_N(A)$	81.9	64.3	55.9	52.6	50.0	34.4	23.6	19.2	
(c) β = 20 cps, d' = 1.3, 1000 trials									
$P_{SN}(A)$	96.3	91.6	88.9	86.8	85.4	78.3	67.6	63.0	
$P_N(A)$	71.7	54.4	49.5	44.2	42.3	29.9	19.6	15.3	

TABLE B-XV

Variable β, $s/b^2 = 1.1$, $S/N = 18$, $T_o = 0.8$ sec

(a) β = 2.5 cps, d' = 1.65, 500 trials									
$P_{SN}(A)$	100.0	98.2	97.2	96.6	96.4	91.6	66.2	76.2	68.8
$P_N(A)$	88.4	67.2	58.8	53.8	50.6	36.6	12.0	16.4	14.2
(b) β = 5 cps, d' = 1.92, 500 trials									
$P_{SN}(A)$	99.0	95.6	93.2	91.6	89.8	83.4	57.4	69.2	63.4
$P_N(A)$	62.8	39.6	31.4	28.0	25.6	17.8	4.2	7.8	5.8
(c) β = 20 cps, d' = 2.28, 1000 trials									
$P_{SN}(A)$	99.0	96.9	96.6	95.5	94.8	93.1	81.8	86.3	84.1
$P_N(A)$	67.8	47.3	41.4	35.8	33.4	26.5	6.4	11.4	8.5
(d) β = 40 cps, d' = 2.37, 1000 trials									
$P_{SN}(A)$	98.0	95.1	93.7	91.8	91.1	88.7	72.6	79.2	76.0
$P_N(A)$	46.9	26.2	20.6	18.0	17.2	13.3	3.0	4.9	3.6

REFERENCES

1. Peterson, W. W., and Birdsall, T. G., "Signal Detection with a Panoramic Receiver," Electronic Defense Group Technical Report No. 38, June 1955.

2. Batten, H. W., Jorgensen, R. A., Macnee, A. B., and Peterson, W. W., "The Response of a Panoramic Receiver to CW and Pulse Signals," Electronic Defense Group Technical Report No. 3, June 1952.

3. Peterson, W. W., and Birdsall, T. G., "The Theory of Signal Detectability," Electronic Defense Group Technical Report No. 13, June 1953.

4. Tanner, Jr., W. P., "Definitions of d' and η as Psychophysical Measures," Electronic Defense Group Technical Report No. 80, March 1958.

DISTRIBUTION LIST

Copy No.	
1-2	Commanding Officer, U. S. Army Signal Research and Development Laboratory, Fort Monmouth, New Jersey, ATTN: Senior Scientist, Countermeasures Division
3	Commanding General, U. S. Army Electronic Proving Ground, Fort Huachuca, Arizona, ATTN: Director, Electronic Warfare Department
4	Chief, Research and Development Division, Office of the Chief Signal Officer, Department of the Army, Washington 25, D. C., ATTN: SIGEB
5	Chief, Plans and Operations Division, Office of the Chief Signal Officer, Washington 25, D. C., ATTN: SIGEW
6	Commanding Officer, Signal Corps Electronics Research Unit, 9560th USASRU, P. O. Box 205, Mountain View, California
7	U. S. Atomic Energy Commission, 1901 Constitution Avenue, N. W., Washington 25, D. C., ATTN: Chief Librarian
8	Director, Central Intelligence Agency, 2430 E Street, N. W., Washington 25, D. C., ATTN: OCD
9	Signal Corps Liaison Officer, Lincoln Laboratory, Box 73, Lexington 73, Massachusetts, ATTN: Col. Clinton W. Janes
10-19	Commander, Armed Services Technical Information Agency, Arlington Hall Station, Arlington 12, Virginia, ATTN: TIPDR
20	Commander, Air Research and Development Command, Andrews Air Force Base, Washington 25, D. C., ATTN: RDTC
21	Directorate of Research and Development, USAF, Washington 25, D. C., ATTN: Chief, Electronic Division
22-23	Commander, Wright Air Development Center, Wright-Patterson Air Force Base, Ohio ATTN: WCOSI-3
24	Commander, Wright Air Development Center, Wright-Patterson Air Force Base, Ohio, ATTN: WCLGL-7
25	Commander, Air Force Cambridge Research Center, L. B. Hanscom Field, Bedford, Massachusetts, ATTN: CROTLR-2
26	Commander, Rome Air Development Center, Griffiss Air Force Base, New York, ATTN: RCSSLD
27	Commander, Air Proving Gound Center, ATTN: Adj/Technical Report Branch, Eglin Air Force Base, Florida
28	Commander, Special Weapons Center, Kirtland Air Force Base, Albuquerque, New Mexico
29	Chief, Bureau of Ordnance, Code ReO-1, Department of the Navy, Washington 25, D. C.
30	Chief of Naval Operations, EW Systems Branch, OP-347, Department of the Navy, Washington 25, D. C.
31	Chief, Bureau of Ships, Code 840, Department of the Navy, Washington 25, D.C.
32	Chief, Bureau of Ships, Code 843, Department of the Navy, Washington 25, D.C.
33	Chief, Bureau of Aeronautics, Code EL-8, Department of the Navy, Washington 25, D. C.
34	Commander, Naval Ordnance Test Station, Inyokern, China Lake, California, ATTN: Test Director-Code 30
35	Commander, Naval Air Missile Test Center, Point Mugu, California, ATTN: Code 366
36	Director, Naval Research Laboratory, Countermeasures Branch, Code 5430, Washington 25, D. C.
37	Director, Naval Research Laboratory, Washington 25, D. C., ATTN: Code 2021
38	Director, Air University Library, Maxwell Air Force Base, Alabama, ATTN: CR-4987
39	Commanding Officer-Director, U. S. Naval Electronic Laboratory, San Diego 52, California
40	Office of the Chief of Ordnance, Department of the Army, Washington 25, D. C., ATTN: ORDTU
41	Chief, West Coast Office, U. S. Army Signal Research and Development Laboratory, Bldg. 6, 75 S. Grand Avenue, Pasadena 2, California
42	Commanding Officer, U. S. Naval Ordnance Laboratory, Silver Springs 19, Maryland
43-44	Chief, U. S. Army Security Agency, Arlington Hall Station, Arlington 12, Virginia, ATTN: GAS-24L

DISTRIBUTION LIST (Cont'd)

Copy No.	
45	President, U. S. Army Defense Board, Headquarters, Fort Bliss, Texas
46	President, U. S. Army Airborne and Electronics Board, Fort Bragg, North Carolina
47	U. S. Army Antiaircraft Artillery and Guided Missile School, Fort Bliss, Texas, ATTN: E and E Department
48	Commander, USAF Security Service, San Antonio, Texas, ATTN: CLR
49	Chief of Naval Research, Department of the Navy, Washington 25, D. C., ATTN: Code 931
50	Commanding Officer, U. S. Army Security Agency, Operations Center, Fort Huachuca, Arizona
51	President, U. S. Army Security Agency Board, Arlington Hall Station, Arlington 12, Virginia
52	Operations Research Office, Johns Hopkins University, 6935 Arlington Road, Bethesda 14, Maryland, ATTN: U. S. Army Liaison Officer
53	The Johns Hopkins University, Radiation Laboratory, 1315 St. Paul Street, Baltimore 2, Maryland, ATTN: Librarian
54	Stanford Electronics Laboratories, Stanford University, Stanford, California, ATTN: Applied Electronics Laboratory Document Library
55	HRB-Singer, Inc., Science Park, State College, Penna., ATTN: R. A. Evans, Manager, Technical Information Center
56	ITT Laboratories, 500 Washington Avenue, Nutley 10, New Jersey, ATTN: Mr. L. A. DeRosa, Div. R-15 Lab.
57	The Rand Corporation, 1700 Main Street, Santa Monica, California, ATTN: Dr. J. L. Hult
58	Stanford Electronics Laboratories, Stanford University, Stanford, California, ATTN: Dr. R. C. Cumming
59	Willow Run Laboratories, The University of Michigan, P. O. Box 2008, Ann Arbor, Michigan, ATTN: Dr. Boyd
60	Stanford Research Institute, Menlo Park, California, ATTN: Dr. Cohn

Copy No.	
61-62	Commanding Officer, U. S. Army Signal Missile Support Agency, White Sands Missile Range, New Mexico, ATTN: SIGWS-EW and SIGWS-FC
63	Commanding Officer, U. S. Naval Air Development Center, Johnsville, Pennsylvania, ATTN: Naval Air Development Center Library
64	Commanding Officer, U. S. Army Signal Research and Development Laboratory, Fort Monmouth, New Jersey, ATTN: U. S. Marine Corps Liaison Office, Code AO-4C
65	President, U. S. Army Signal Board, Fort Monmouth, New Jersey
66-76	Commanding Officer, U. S. Army Signal Research and Development Laboratory, Fort Monmouth, New Jersey ATTN: 1 Copy - Director of Research 1 Copy - Technical Documents Center ADT/E 1 Copy - Chief, Ctms Systems Branch, Countermeasures Division 1 Copy - Chief, Detection and Location Branch, Countermeasures Division 1 Copy - Chief, Jamming and Deception Branch, Countermeasures Division 1 Copy - File Unit No. 4, Mail and Records, Countermeasures Division 1 Copy - Chief, Vulnerability Br., Electromagnetic Environment Division 1 Copy - Reports Distribution Unit, Countermeasures Division File 3 Cpys - Chief, Security Division (for retransmittal to BJSM)
77	Director, National Security Agency, Ft. George G. Meade, Maryland, ATTN: TEC
78	Dr. H. W. Farris, Director, Electronic Defense Group, University of Michigan Research Institute, Ann Arbor, Michigan
79-99	Electronic Defense Group Project File University of Michigan Research Institute, Ann Arbor, Michigan
100	Project File, University of Michigan Research Institute, Ann Arbor, Michigan

Above distribution is effected by Countermeasures Division, Surveillance Dept., USASRDL, Evans Area, Belmar, New Jersey. For further information contact Mr. I. O. Myers, Senior Scientist, telephone PRospect 5-3000, Ext. 61252.